Modulation of glycine potency in rat recombinant NMDA receptors containing chimeric NR2A/2D subunits expressed in *Xenopus laevis* oocytes

Philip E. Chen[1], Matthew T. Geballe[2], Elyse Katz[3], Kevin Erreger[3], Matthew R. Livesey[1], Kate K. O'Toole[3], Phuong Le[3], C. Justin Lee[3], James P. Snyder[2], Stephen F. Traynelis[3] and David J. A. Wyllie[1]

[1]*Centre for Neuroscience Research, University of Edinburgh, Hugh Robson Building, George Square, Edinburgh EH8 9XD, UK*
[2]*Department of Chemistry, Emory University, 1515 Dickey Drive, Atlanta, GA 30322, USA*
[3]*Department of Pharmacology, Emory University School of Medicine, Rollins Research Center, 1510 Clifton Road, Atlanta, GA 30322, USA*

Heteromeric NMDARs are composed of coagonist glycine-binding NR1 subunits and glutamate-binding NR2 subunits. The majority of functional NMDARs in the mammalian central nervous system (CNS) contain two NR1 subunits and two NR2 subunits of which there are four types (A–D). We show that the potency of a variety of endogenous and synthetic glycine-site coagonists varies between recombinant NMDARs such that the highest potency is seen at NR2D-containing and the lowest at NR2A-containing NMDARs. This heterogeneity is specified by the particular NR2 subunit within the NMDAR complex since the glycine-binding NR1 subunit is common to all NMDARs investigated. To identify the molecular determinants responsible for this heterogeneity, we generated chimeric NR2A/2D subunits where we exchanged the S1 and S2 regions that form the ligand-binding domains and coexpressed these with NR1 subunits in *Xenopus laevis* oocytes. Glycine concentration–response curves for NMDARs containing NR2A subunits including the NR2D S1 region gave mean glycine EC_{50} values similar to NR2A(WT)-containing NMDARs. However, receptors containing NR2A subunits including the NR2D S2 region or both NR2D S1 and S2 regions gave glycine potencies similar to those seen in NR2D(WT)-containing NMDARs. In particular, two residues in the S2 region of the NR2A subunit (Lys719 and Tyr735) when mutated to the corresponding residues found in the NR2D subunit influence glycine potency. We conclude that the variation in glycine potency is caused by interactions between the NR1 and NR2 ligand-binding domains that occur following agonist binding and which may be involved in the initial conformation changes that determine channel gating.

(Received 20 August 2007; accepted after revision 23 October 2007; first published online 25 October 2007)

Corresponding author D. J. A. Wyllie: Centre for Neuroscience Research, Hugh Robson Building, University of Edinburgh, George Square, Edinburgh EH8 9XD, UK.   Email: dwyllie1@staffmail.ed.ac.uk

In the mammalian central nervous system (CNS), NMDARs are heteromeric glutamate receptor–channels predominantly composed of two NR1 and two NR2 subunits, of which there are four subtypes (NR2A–D). These receptors mediate the 'slow' component of the excitatory postsynaptic current in neurones and have been implicated in various physiological and pathophysiological processes in the CNS. In contrast to the ubiquitously expressed NR1 subunit, the expression of the NR2 subunit is regulated temporally and spatially within the mammalian brain. These NR2 subunits impart a variety of distinct biophysical and pharmacological properties on the NMDAR complex that characterize different NMDAR subtypes (for reviews see Dingledine *et al.* 1999; Cull-Candy *et al.* 2001; Erreger *et al.* 2004). In addition, there are NR3A and B subunits that are thought to assume a modulatory role within the NMDAR complex. Each subunit is composed of a number of specific functional regions: an amino-terminal domain, which is the site of action for a number of modulatory agents; the ligand-binding domain (LBD); the membrane-associated domains, which form the ion channel pore; and an intracellularly located carboxyl-terminal domain, which allows the receptor to interact with various signalling and scaffolding molecules. A cartoon depiction of the structure of an NMDAR subunit is shown in Fig. 1*A*. Uniquely among ionotropic receptors, NMDARs require

This paper has online supplemental material.

both glutamate and the coagonist, glycine, to bind to the receptor for channel activation to occur (Johnson & Ascher, 1987; Kleckner & Dingledine, 1988). The glycine binding site is located on the NR1 subunit and the glutamate binding site on the NR2 subunit (for reviews see Chen & Wyllie, 2006; Mayer, 2006) and they are formed by residues encoded by regions within the subunit cDNA, a region (S1) preceding the first membrane-spanning domain and a region (S2) between the second and third membrane-spanning domains. A comparison of the amino acid sequences of these two regions in NR2A and NR2D NMDAR subunits is shown in
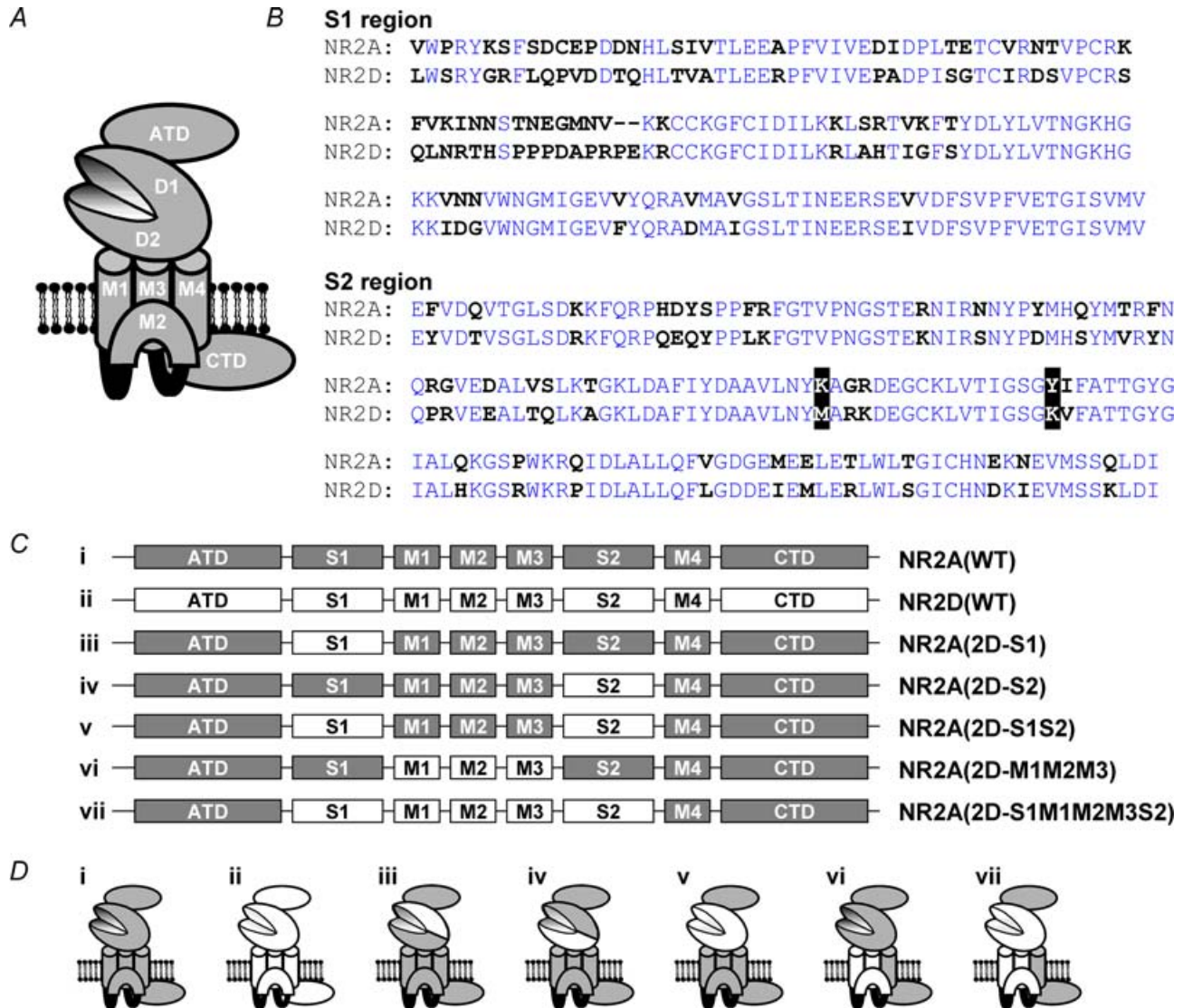

Figure 1. Outline structure of an NMDAR subunit, sequences of the S1 and S2 regions in NR2A and NR2D NMDAR subunits and pictorial representation of the various chimeras investigated

A, cartoon sketch of an ionotropic glutamate receptor subunit showing the proposed membrane topology of three membrane spanning domains (M1, M3 and M4) and a re-entrant loop (M2) and the location of the amino terminal domain (ATD) and carboxy terminal domain (CTD). The ligand binding domains (denoted D1 and D2) are formed by the S1 and S2 regions of the protein which come together to form a hinged clamshell-like structure. *B*, amino acid sequence of the S1 and S2 regions of NR2A and NR2D NMDAR subunits. The S1 region contains amino acids that contribute mainly, but not exclusively, to Domain1 of the ligand-binding site, while those in S2 contribute mainly, but not exclusively, to Domain2 of the ligand-binding site. Amino acids which are different in NR2A and NR2D NMDAR subunits are highlighted in bold. *C*, linear representation of wild-type NR2A and NR2D NMDAR subunits. The main structural-forming domains are shown in grey for NR2A and white for NR2D NMDAR subunits. The various chimeric subunits that have been investigated in this study are shown together with the source of each of the domains in the chimeric subunits and the nomenclature used to describe them. *D*, cartoon representation of the constructs (i–vii, shown in *C*) illustrating how the various functional domains from the NR2D subunit are incorporated into the five chimeric subunits investigated in this study.

Fig. 1*B* while a comparison of the sequences of the S1 and S2 regions for all four NR2 NMDARs is shown in the online supplemental material, Supplemental Fig. 1. Recently, X-ray crystallography has resolved the structures of the glutamate and glycine binding pockets from the NR2A and NR1 subunits and has found that in the NR1–NR2A S1S2 heterodimer both glutamate and glycine binding pockets assemble in a 'back-to-back' configuration (Furukawa & Gouaux, 2003; Furukawa *et al.* 2005). Since the initial cloning of the NMDAR subunits, it has been observed that glutamate potency differs among the NMDAR subtypes (Kutsuwada *et al.* 1992; Ikeda *et al.* 1992; Monyer *et al.* 1992; Laurie & Seeburg, 1994; Erreger *et al.* 2007). The largest difference in glutamate potency is seen between NR2A- and NR2D-containing NMDARs where glutamate EC_{50} values vary by up to one order of magnitude. Indeed this difference in potency is observed for a large number of ligands acting at the NR2 binding site (Erreger *et al.* 2007). Similarly, the four types of heterodimeric NMDARs also show variation in the potency with which glycine acts at the NR1 coagonist binding site. Intriguingly, a 10-fold variation in glycine potency is also seen with NR2A- or NR2D-containing NMDARs (Kuryatov *et al.* 1994; Wafford *et al.* 1995; Furukawa & Gouaux, 2003). Furthermore, it is known that binding of glutamate to its NR2 binding site influences the binding of glycine to its NR1 binding site and *vice versa* (for example see Vyklicky *et al.* 1990; Benveniste *et al.* 1990; Benveniste & Mayer, 1991; Kemp & Priestley, 1991; Lester *et al.* 1993; Priestley & Kemp, 1994; Regalado *et al.* 2001). Nevertheless, the overall potency (EC_{50}) with which an agonist acts is determined not only by equilibrium constants governing binding reactions but also by the rate constants controlling subsequent downstream channel gating (including desensitization) (see Colquhoun, 1998). Thus, differences in glycine potency at each of the four NMDAR subtypes will be influenced not only by the equilibrium constant for binding to the NR1 subunit but also by the extent to which the NR1 NMDAR subunit interacts with NR2 NMDAR subunits as part of the channel gating process.

In order to understand the molecular determinants underlying differences in glycine-site potency at NMDAR subtypes, we have characterized the potencies of endogenous and synthetic ligands that act at the NR1 coagonist binding site and have examined the pharmacology of recombinant NMDARs expressing chimeric receptors composed of regions from either NR2A or NR2D subunits. Specifically, we have observed that the S2 region that forms the majority of Domain2 of the LBD from the NR2D subunit is a major structural determinant of glycine potency. We have identified two residues in NR2A NMDAR subunits that when mutated to those found in NR2D NMDAR subunits result in a NR1/NR2D NMDAR-like glycine potency. We contend that interactions between

NR1 and NR2 LBDs that occur following agonist binding and influence the channel-gating process are responsible for the differences in glycine potencies observed at the various NMDAR subtypes. Thus, distinct pharmacological properties of different NMDAR subtypes are not only dependent on the distinct intrasubunit binding pockets (e.g. Chen *et al.* 2005; Erreger *et al.* 2007), but may also be specified by interdomain interactions between the LBDs. In an accompanying paper (Wrighton *et al.* 2008) we show that the LBD, in addition to its effect on influencing glycine potency, contributes to the potency of voltage-dependent Mg^{2+} block at NMDARs.

Methods

Plasmid constructs, cRNA synthesis and receptor expression in oocytes

The amino acid numbering system we use here is consistent with our previous publications investigating structure–function relationships in recombinant NMDARs and refers to the position of residues in the mature protein (i.e. residues up to and including Ala18 in NR1, Arg19 in NR2A and Ala23 in NR2D are excluded in our numbering system). The wild-type pSP64T-derived expression plasmids for rodent NR1 and NR2 NMDA receptor subunits were as previously described (Chen *et al.* 2005; Wyllie *et al.* 2006). In this study we coexpressed various NR2 receptor subunits with the NR1–1a (exon 5 lacking, exon 21, 22 containing) subunit (Hollmann *et al.* 1993), which we will refer to as 'NR1'. Chimeras between NR2A and NR2D subunits (shown as constructs (i) and (ii) in Fig. 1*C* and *D*, respectively) were introduced using a PCR-based strategy. Chimeric NR2A/D subunits were generated by replacing Val370–Val518 in the NR2A subunit with Leu389–Val539 from the NR2D subunit (referred to as the NR2A(2D-S1) chimera; shown as construct (iii) in Fig. 1*C* and *D*) and by replacing Glu638–Ile795 in the NR2A subunit with Glu659–Ile816 from the NR2D subunit (referred to as the NR2A(2D-S2) chimera; shown as construct (iv) in Fig. 1*C* and *D*). A chimera that replaced the NR2A S1 and S2 regions with the equivalent sequences from the NR2D subunit is referred to as NR2A(2D-S1S2) and shown as construct (v) in Fig. 1*C* and *D*. In addition to these 'binding site' chimeras, we also generated a chimera in which the NR2A M1, M2 and M3 membrane associated regions (residues Ser519–Glu638) were replaced by those found in the NR2D subunit (Arg541–Glu658). We refer to this chimera as NR2A(2D-M1M2M3) and it is shown as construct (vi) in Fig. 1*C* and *D*. Finally the NR2A(2D-S1M1M2M3S2) chimera replaced both the NR2A ligand-binding domain and first three membrane-associated regions with those found in the NR2D subunit

(shown as construct (vii) in Fig. 1*C* and *D*). All inserted PCR-generated DNA segments and subcloning sites were confirmed by DNA sequencing. Site-directed mutagenesis was performed using PCR-based strategies and verified by sequencing. cRNA was synthesized as runoff transcripts from restriction endonuclease (*Mlu*I or *Not*I) linearized plasmid DNA using the Promega RiboMax RNA synthesis kit (Promega, Madison, WI) or mMessage Machine (Ambion, Warrington, UK). Reactions were supplemented with 0.75 mM capping nucleotide $m^7G(5')ppp(5')G$ (Promega) in the presence of 1.6 mM GTP. cRNA amounts and integrity were estimated by intensity of fluorescence in ethidium bromide-stained agarose gels. NR1 and NR2 cRNAs were mixed at a nominal ratio ranging from between 1 : 1 and 1 : 9, with NR1 content being 5 ng.

Stage V–VI oocytes were obtained from *Xenopus laevis* that had been anaesthetized by immersion in a solution of 3-amino-benzoic acid ethylester (0.5%) and then killed by injection of an overdose solution of pentobarbital (0.4 ml of 20% solution) followed by decapitation and exsanguation after the confirmation of loss of cardiac output, for experiments carried out at the University of Edinburgh. For experiments carried out at Emory University, oocytes were obtained from a ovarian lobe that had been surgically removed from *Xenopus laevis* anaesthetized with 3-amino-benzoic acid ethylester (Traynelis *et al.* 1998; Chen *et al.* 2005). All procedures were carried out in accordance with current UK Home Office requirements and the Emory University IACUC. Prior to injection with cRNA mixtures of interest, the follicular membranes of the oocytes were removed. After injection oocytes were placed in separate wells of 24-well plates containing a modified Barth's solution with composition (mM): NaCl 88, KCl 1, NaHCO$_3$ 2.4, MgCl$_2$ 0.82, CaCl$_2$ 0.77, Tris-Cl 15, adjusted to pH 7.35 with NaOH (Sigma-Aldrich, UK). This solution was supplemented with 50 IU ml^{-1} penicillin and 50 μg ml^{-1} streptomycin (Invitrogen, UK). Oocytes were placed in an incubator (19°C) for 24–48 h to allow for receptor expression and then stored at 4°C until required for electrophysiological measurements.

Electrophysiological recordings and solutions

Two electrode voltage clamp (TEVC) recordings were made using a GeneClamp 500 or OC-725 amplifier (Molecular Devices, Union City, CA, USA; Warner Instruments, Hamden, CT, USA), from oocytes that were placed in a solution that contained (mM) either: NaCl 115, KCl 2.5, Hepes 10, BaCl$_2$ 1.8, EDTA 0.01, pH 7.3 with NaOH (20°C) for experiments carried out at the University of Edinburgh, or NaCl 90, KCl 3, Hepes 5, BaCl$_2$ 0.5, EDTA 0.01, pH 7.3 with NaOH (20°C) for experiments carried out at Emory University. The use of

either set of solutions resulted in comparable estimates for agonist potencies and the data obtained from experiments undertaken at either institution were pooled. Chemicals were purchased from Sigma-Aldrich (Poole, UK or St Louis, MO, USA). EDTA (10 μM) was added to chelate contaminant extracellular divalent ions, including trace amounts of Zn^{2+}. Current and voltage electrodes were made from thin-walled borosilicate glass (GC150TF-7.5, Harvard Apparatus, Kent, UK) using a PP-830 electrode puller (Narashige Instruments, Japan) and when filled with 3 M KCl they possessed resistances of between 0.5 and 1.5 MΩ. Oocytes were voltage-clamped at −40 mV. For L-glutamate concentration–response measurements, the recording solution was further supplemented with 50 μM glycine and for glycine dose–response measurements this solution was supplemented with 50 μM glutamate or 30 μM homoquinolinic acid. Application of solutions was controlled either manually or through user-written software controlling a rotary valve. Data were filtered at 10 Hz and digitized at 100 Hz. Test solutions were applied for 20–60 s or until a plateau to the agonist-evoked response had been achieved. When investigating the actions of various agonists acting at the coagonist binding site on the NR1 subunit we use the term 'relative efficacy' to indicate the size of the maximum response evoked by a ligand relative to the response to a saturating concentration of glycine (nominally set to equal 100%; see Erreger *et al.* 2007). Such relative efficacies can only be compared within, and not between, different NMDAR subtypes or chimeras since the maximum open probability of an NMDAR is subunit dependent, as has been shown from single-channel studies (Wyllie *et al.* 1998; Banke & Traynelis, 2003; Popescu & Auerbach, 2003; Erreger *et al.* 2005*a*,*b*; Schorge *et al.* 2005). Glutamate- and glycine-site agonists and antagonists were purchased from Tocris Bioscience (Bristol, UK or Ellisville, MO, USA).

Data analysis for dose–response curves

Concentration–response curves were fitted individually for each oocyte with the Hill equation:

$$I = I_{\max}/\bigl(1 + (\mathrm{EC}_{50}/[\mathrm{A}])^{n_{\mathrm{H}}}\bigr)$$

where n_{H} is the Hill coefficient, $I_{\max}$ is the maximum current, [A] is the concentration of agonist, and EC$_{50}$ is the concentration of agonist that produces a half-maximum response. Each data point was then normalized to the fitted maximum of the dose–response curve. The normalized values were then pooled and averaged for each construct and fitted again with the Hill equation, with the maximum and minimum for each curve being constrained to asymptote to 1 and 0, respectively. A similar protocol was used to determine the concentration of the NMDA-glycine site antagonist 5,7-dichlorokynurenic acid (5,7-DCKA) required to inhibit a glycine-evoked response by 50%

(IC_{50}). In these experiments the glycine concentration was set to the concentration required to evoke a half-maximal response in each of the constructs being investigated. Throughout this study we use the term 'potency' to describe the relative differences in EC_{50} or IC_{50} values for ligands acting at the various NMDAR constructs we have investigated. Thus increases in potency correspond to decreases in EC_{50} (or IC_{50}) values and *vice versa*. The level of 'contaminating' glycine in our recording solutions was determined using the method described by Johnson & Ascher (1992) and Traynelis *et al.* (1995). We estimated these levels to be < 10 nM.

Measurement of competitive antagonist equilibrium binding constants using Schild analysis

5,7-DCKA antagonism on wild-type NR2A-, NR2D- and NR2A(2D-S1S2)-containing NMDARs was also examined using the Schild method (Arunlakshana & Schild, 1959; Wyllie & Chen, 2007). Partial, concentration–response curves were obtained from two concentrations ($<< EC_{50}$) of glycine in the absence of antagonist. Then, partial concentration–response curves were determined in the presence of increasing concentrations of 5,7-DCKA, by applying higher concentrations of glycine in order to produce approximately equivalent responses. 5,7-DCKA was preapplied for 120 s before glycine application in order to ensure that the antagonist was in equilibrium with the receptors. As predicted by the low concentration limit of the Hill equation, these partial concentration–response curves produced a series of straight lines when plotted on a log–log scale and the slope of the initial (antagonist-free) curve was fitted on the remaining two-point concentration–response curves, generating a series of parallel lines. From these lines the dose ratio (r, ratio of glycine concentrations needed to produce the same response in the presence and absence of 5,7-DCKA) could be calculated for each 5,7-DCKA concentration used. The mean dose ratios were used to generate a Schild plot, of log ($r - 1$) *versus* log [B], where [B] is the antagonist concentration. In the first instance, the data was fitted as a 'free' fit with a linear regression. The Schild equation, $(r - 1) = [B]/K_B$, predicts that the slope of the Schild plot should be 1 for a competitive antagonist at equilibrium. Therefore if the slope of the 'free' fit was sufficiently close to unity, the data were taken to be consistent with the Schild equation, and the data were refitted with the slope fixed at 1. The intercept on the x-axis of the line with a fixed slope of 1 gives the log of the equilibrium constant for antagonist binding, K_B (see Wyllie & Chen, 2007).

Molecular modelling

Starting from the crystal structure of the NR1/NR2A agonist binding domain dimer (PDB code 2A5T), a model of the NR2D glutamate binding domain has been constructed as previously described (Erreger *et al.* 2007). Agonist binding domains of NR2A and NR2D show 72% sequence identity and 82% homology in their alignment. The structure of NR2A was modified from that of 2A5T to represent the wild-type peptide sequence, and the models were energy optimized with the OPLS-2005 force field in Maestro (Schrödinger, Portland, OR, USA; Kaminski *et al.* 2001) to remove strain. Subsequently, the glycine and glutamate ligands were left in their crystallographic positions prior to unrestrained molecular dynamics simulation in which both protein and ligand can move. These complexes were then prepared for molecular dynamics (MD) simulation as previously described (Erreger *et al.* 2007). After a 50 ps simulation with ligand and protein restrained to allow for water equilibration, a 10 ps simulation was performed at 50 K to remove any gross steric clashes within the structures. The simulation was then restarted at 50 K and the temperature was increased linearly to 300 K over 250 ps (1 K ps^{-1}) and continued at 300 K for 10 ns. All MD simulations were performed with NPT conditions (Erreger *et al.* 2007), while the corresponding figures were produced using Visual Molecular Dynamics (VMD; Humphrey *et al.* 1996).

Results

Glycine-site agonist potencies at heterodimeric NR1/NR2 NMDARs

We initially investigated the potencies of a series of glycine-site agonists at NR1/NR2A, NR1/NR2B, NR1/NR2C and NR1/NR2D NMDARs. These included endogenous ligands such as glycine, D- and L-isomers of serine and alanine and synthetic halogenated and cyclic derivatives that also act as coagonists at the NR1 NMDAR subunit. Figure 2 illustrates TEVC currents recorded from oocytes expressing either NR1/NR2A (Fig. 2*A*) or NR1/NR2D (Fig. 2*B*) NMDARs. The currents were evoked by applying (cumulatively) increasing concentrations of glycine in the presence of a saturating concentration of glutamate (50 μM). Figure 2*C* shows the mean data points obtained for each of the four receptor subtypes which have been fitted with the Hill equation. As is shown in Fig. 2*C* and in the summary data from all our experiments (Fig. 3) all agonists studied displayed the same rank order of potency, regardless of their relative efficacy or structure. Thus, the order of potency for all agonists is (highest potency, lowest EC_{50}) NR2D > NR2C > NR2B > NR2A (lowest potency, highest EC_{50}). Differences in potency ratios between NR2A- and NR2D-containing NMDARs ranged between 8-fold (D-serine) and 28-fold (β-fluoro-DL-alanine). When comparing relative efficacies, where glycine was denoted a value of 100% (see Methods), we can see

that most of the ligands studied were in the range of ∼80–110% of this value. The determination of a particular ligand's 'relative efficacy' or 'potency' does not provide us with any direct measure of equilibrium constants underlying either binding or gating reactions (Colquhoun, 1998). Indeed measurements of macroscopic responses are in general difficult to interpret in terms of the underlying rate constants that are altered as a result of different ligands being used to activate a receptor without additional information that can be obtained from single-channel studies (for example see Erreger *et al.* 2005*b*). Nevertheless mutations in the ligand binding site of NR2A and NR2D NMDAR subunits that lead to 1000-fold shifts in glutamate's potency can be accounted for by changes in the dissociation rate constant (Wyllie *et al.* 2006) suggesting distinct functional domains within the NMDAR may influence binding and gating reactions separately (see Gibb, 2006). Therefore since the greatest difference in potency of ligands acting at the glycine site is seen with NR2A- and NR2D-containing NMDARs, we have investigated which structural elements contained within these two NR2 subunits might be responsible for the observed difference in agonist potencies at the ligand-binding site in the NR1 subunit.
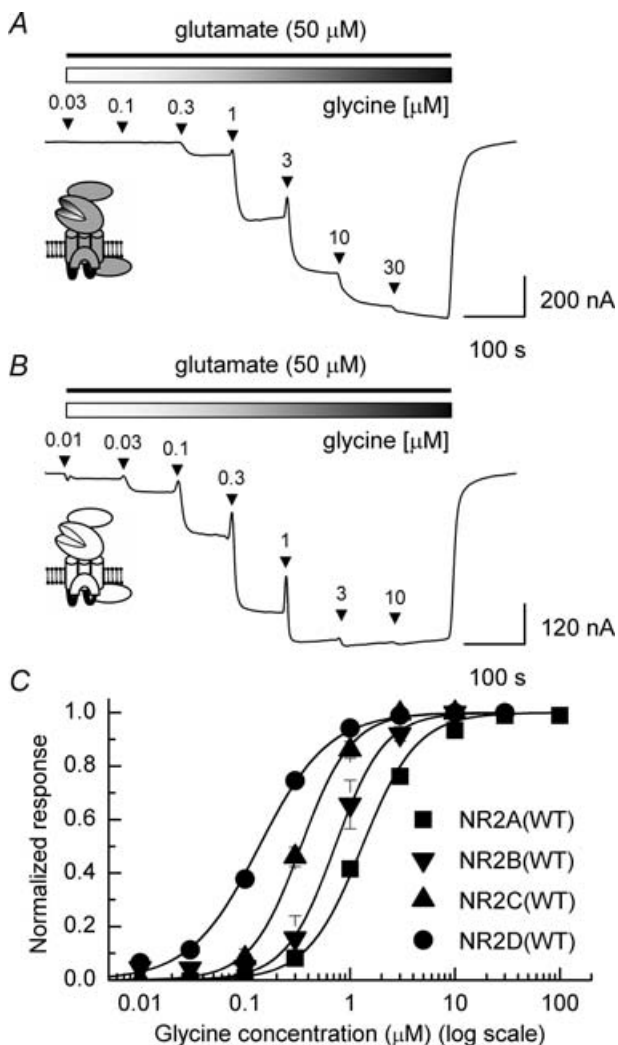

Figure 2. Example TEVC current traces showing responses evoked by increasing concentrations of glycine for NR1/NR2A and NR1/NR2D NMDARs

A, example TEVC current recording obtained from an oocyte expressing NR1/NR2A(WT) NMDARs. In the presence of glutamate (50 μM), increasing concentrations of glycine (30 nM to 30 μM) were applied cumulatively. *B*, as *A* but recorded from an oocyte expressing NR1/NR2D(WT) NMDARs and with the range of glycine concentrations applied being 10 nM to 10 μM. Note the increased glycine potency at NR2D-containing compared to NR2A-containing NMDARs. *C*, mean glycine concentration–response curves for each of the four NMDAR subtypes. The rank order of glycine potency (highest potency, lowest EC_{50}) is NR2D > NR2C > NR2B > NR2A with the mean EC_{50} values and Hill slopes for each of the NMDAR combinations given in Fig. 3.

Glycine potency at recombinant NMDARs containing chemeric NR2A/D subunits

Several studies have shown that when glutamate binds to NMDARs this causes the rate of dissociation of glycine from its binding site to increase and hence a subsequent reduction in its affinity (for example see, Vyklicky *et al.* 1990; Benveniste *et al.* 1990; Benveniste & Mayer, 1991; Kemp & Priestley, 1991; Lester *et al.* 1993; Priestley & Kemp, 1994; Regalado *et al.* 2001). Thus, we hypothesized that the variation in the potency of coagonists acting at the glycine (NR1) site we see with NR1/NR2A and NR1/NR2D NMDARs may be specified by amino acid residues within the S1 and S2 domains of the NR2 (glutamate binding) since earlier studies have demonstrated glutamate–glycine binding interactions. Although the amino acid residues that hydrogen-bond with glutamate when it occupies the NR2 ligand-binding site are conserved among NR2A and NR2D subunits (Furukawa *et al.* 2005), sequence alignments of the entire S1 and S2 regions show a number of important differences (Fig. 1*B*; Supplemental Fig. 1). In addition, molecular dynamics simulations of NR1/NR2A and NR1/NR2D suggest additional differences between the NR2 subunit (Erreger *et al.* 2007). We generated three chimeric subunits by inserting the NR2DS1, NR2DS2 and both NR2DS1 and S2 domains into the NR2A subunit using PCR-based mutagenesis, and the schematic location of the NR2A/NR2D domain exchanges are shown in Fig. 1*C* and *D*. *In vitro* transcribed cRNA from all chimeras produced robust glutamate-evoked inward currents when expressed with NR1 cRNA.

We have previously reported the effects on glutamate potency of exchanging S1 and S2 regions in the NR2A subunit with the equivalent region from the NR2D subunit (Erreger *et al.* 2007). Briefly, replacement of either the S1 or S2 region in NR2A with the corresponding NR2D region produces an NMDAR with a glutamate EC_{50} that

is intermediate between that seen with NR2A(WT)- or NR2D(WT)-containing NMDARs. Replacement of both S1 and S2 regions in NR2A subunits with the respective regions from NR2D subunits results in a chimeric NMDAR where glutamate potency is equivalent to that seen in NR2D(WT)-containing NMDARs (Erreger *et al.* 2007).

Recent structural studies have shown that the glycine and glutamate binding pockets on the NR1 and NR2 subunits interact via their hinge regions in a 'back-to-back' manner (Furukawa *et al.* 2005). We examined the effect

these NR2A/D chimeras had on glycine potency by measuring glycine concentration–response curves in the presence of a saturating concentration of glutamate (50 μM). Figure 4 shows voltage clamp currents recorded in response to the application of 30 nM, 300 nM, 3 μM and 30 μM glycine from oocytes expressing NR1/NR2A (Fig. 4*A*), NR1/NR2D (Fig. 4*B*) or NR1/NR2A(2D-S1S2) (Fig. 4*C*) NMDARs. Mean concentration–response curves for these receptor combinations and the NR2A(2D-S1) and NR2A(2D-S2) chimeras are shown in Fig. 4*D*.

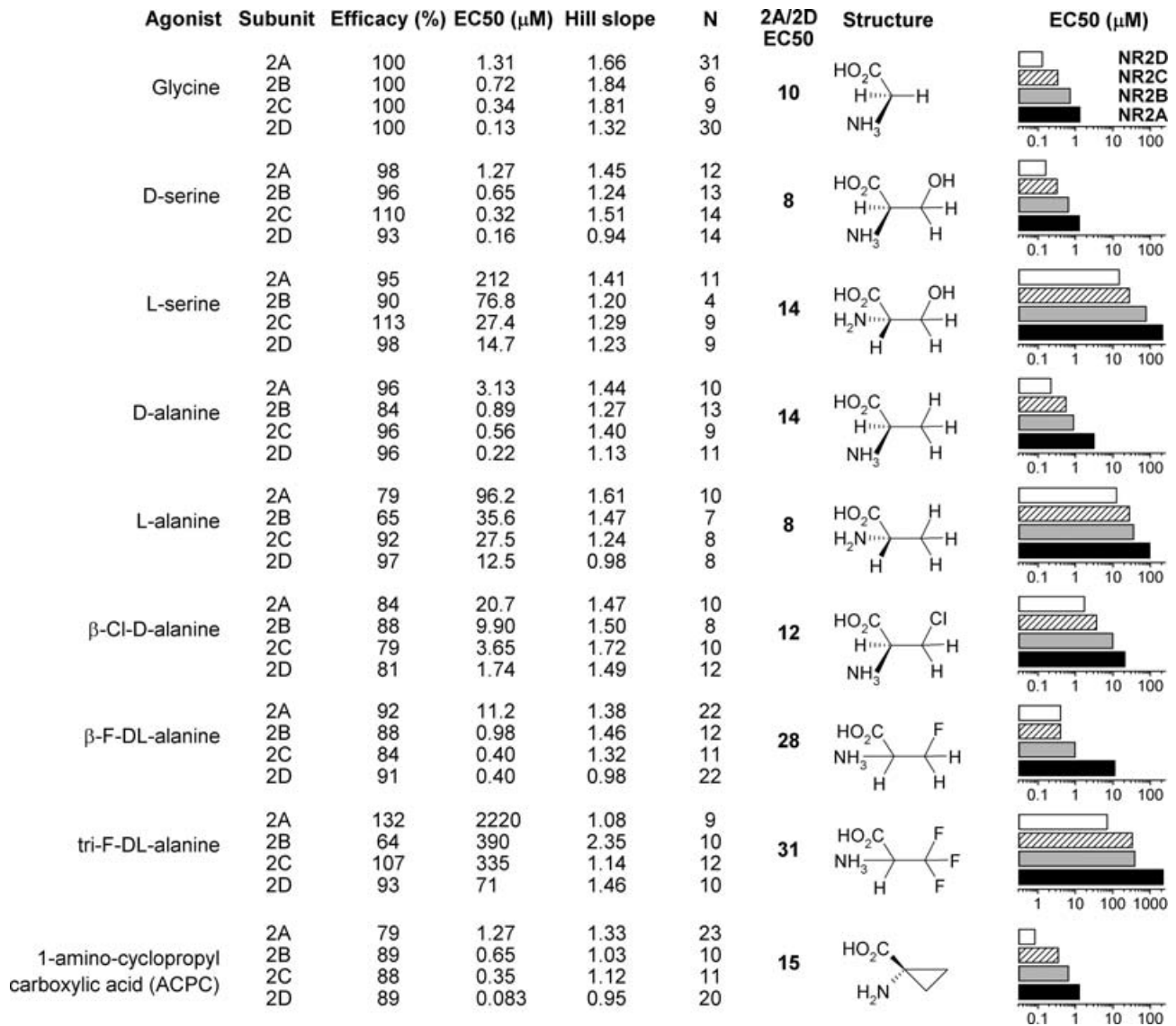| Agonist	Subunit	Efficacy (%)	EC50 (μM)	Hill slope	N	2A/2D EC50	Structure	EC50 (μM)
Glycine	2A	100	1.31	1.66	31	10		
	2B	100	0.72	1.84	6			
	2C	100	0.34	1.81	9			
	2D	100	0.13	1.32	30			
D-serine	2A	98	1.27	1.45	12	8		
	2B	96	0.65	1.24	13			
	2C	110	0.32	1.51	14			
	2D	93	0.16	0.94	14			
L-serine	2A	95	212	1.41	11	14		
	2B	90	76.8	1.20	4			
	2C	113	27.4	1.29	9			
	2D	98	14.7	1.23	9			
D-alanine	2A	96	3.13	1.44	10	14		
	2B	84	0.89	1.27	13			
	2C	96	0.56	1.40	9			
	2D	96	0.22	1.13	11			
L-alanine	2A	79	96.2	1.61	10	8		
	2B	65	35.6	1.47	7			
	2C	92	27.5	1.24	8			
	2D	97	12.5	0.98	8			
β-Cl-D-alanine	2A	84	20.7	1.47	10	12		
	2B	88	9.90	1.50	8			
	2C	79	3.65	1.72	10			
	2D	81	1.74	1.49	12			
β-F-DL-alanine	2A	92	11.2	1.38	22	28		
	2B	88	0.98	1.46	12			
	2C	84	0.40	1.32	11			
	2D	91	0.40	0.98	22			
tri-F-DL-alanine	2A	132	2220	1.08	9	31		
	2B	64	390	2.35	10			
	2C	107	335	1.14	12			
	2D	93	71	1.46	10			
1-amino-cyclopropyl carboxylic acid (ACPC)	2A	79	1.27	1.33	23	15		
	2B	89	0.65	1.03	10			
	2C	88	0.35	1.12	11			
	2D	89	0.083	0.95	20			

Figure 3. Summary of the potencies and 'relative efficacies' of ligands acting at the NR1 coagonist binding site for each of the four heterodimeric NMDARs

Mean EC$_{50}$ and Hill slope values obtained from fitting concentration–response relationships for a series of NR1 agonists. Efficacy denotes the maximal current response to the test agonist relative to the maximal response to glycine. The ratio of the EC$_{50}$ at NR1/NR2A compared to NR1/NR2D NMDARs is given to indicate the agonist selectivity between these two NMDAR subtypes. The structures of the various agonists are also illustrated together with the subunit dependence of the EC$_{50}$ for each agonist. Notice that for each agonist studied, greatest potency is seen at NR2D-containing NMDARs and the least at NR2A-containing NMDARs.

As reported previously, glycine is approximately 10-fold more potent at NR1/NR2D-containing receptors ($EC_{50} = 133 \pm 7$ nM) than those containing NR2A ($EC_{50} = 1.31 \pm 0.08\,\mu$M). Glycine potency of NMDARs containing the NR2A(2D-S1) chimera

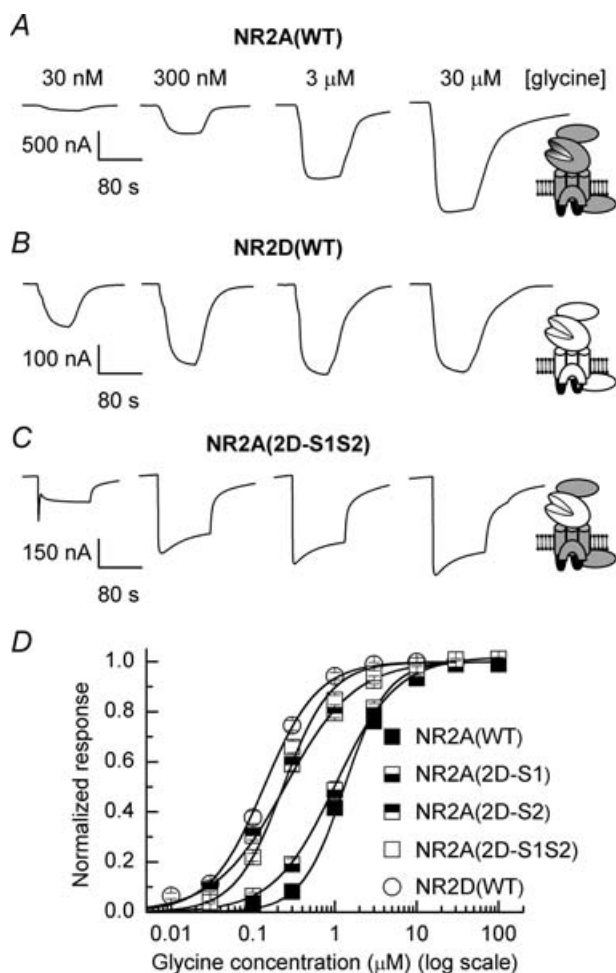($EC_{50} = 1.02 \pm 0.06\,\mu$M) is close to the NR1/NR2A NMDAR value. However, the NR2A(2D-S2) and NR2A(2D-S1S2) chimeras each show glycine potencies close to that of NR2D(WT) receptors (EC_{50} values 219 ± 13 nM and 233 ± 10 nM, respectively). The corresponding Hill slope values for each of these receptor constructs together with the equivalent data for other glycine-site agonists are shown in Fig. 6.

We next examined whether the shift in potency in the NR2A(2D-S1S2) construct was also observed with
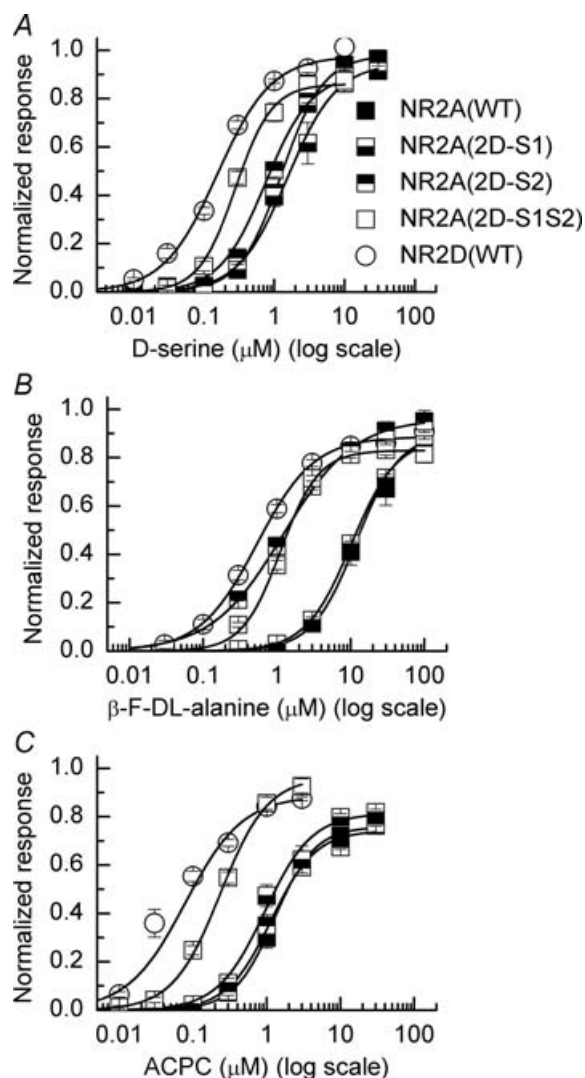

Figure 4. Glycine concentration–response data for wild-type and chimeric NMDARs
A, representative TEVC current recordings obtained from an oocyte expressing NR1/NR2A(WT) NMDARs, elicited by increasing concentrations of glycine (30 nM to 30 μM; in the presence of glutamate (50 μM)). *B*, representative TEVC current recordings obtained from an oocyte expressing NR1/NR2D(WT) NMDARs, elicited by the same concentrations of glycine (and glutamate) as illustrated in *A*. Notice that in contrast to the recordings shown in *A*, responses to 3 μM and 30 μM glycine evoke similarly sized currents indicating that the potency of glycine is greater at NR2D-containing NMDARs. *C*, representative TEVC current recordings obtained from an oocyte expressing NR1/NR2A(2D-S1S2) NMDARs, elicited by the same agonist concentrations as shown in *A* and *B*. *D*, mean concentration–response curves for glycine acting at NR1/NR2A(WT) and NR1/NR2D(WT) NMDARs as well as each of the three 'binding' domain chimeric NMDARs. Mean EC_{50} values and Hill slopes for each of the NMDAR combinations are given in Fig. 6. The mean Hill slopes and mean maximal currents recorded were for NR2A(WT): 1.66 ± 0.08, $1.7 \pm 0.4\,\mu$A; NR2D(WT): 1.32 ± 0.07, $0.4 \pm 0.06\,\mu$A; NR2A(2D-S1): 1.16 ± 0.04, $1.6 \pm 0.2\,\mu$A; NR2A(2D-S2): 0.99 ± 0.04, $2.1 \pm 0.6\,\mu$A; and NR2A(2D-S1S2): 1.48 ± 0.05, $1.9 \pm 0.2\,\mu$A.

Figure 5. Concentration–response curves for D-serine, *β*-fluoro-DL-alanine and ACPC acting at wild-type and chimeric NMDARs
A, mean concentration–response curves for D-serine acting at NR1/NR2A(WT) and NR1/NR2D(WT) NMDARs as well as each of the three chimeric NMDARs. *B*, mean concentration–response curves for *β*-fluoro-DL-alanine. *C*, mean concentration–response curves for ACPC. For each agonist, replacing the S1 and S2 region of the NR2A subunit with the corresponding regions from the NR2D subunit resulted in an increase in agonist potency. Mean EC_{50}, Hill slope and 'relative efficacy' values for each of the agonists acting at the various NMDAR combinations are given in Fig. 6.

other ligands that bind to the NR1 coagonist site. Figure 5 shows the mean concentration–response curves for D-serine (Fig. 5*A*), β-fluoro-DL-alanine (Fig. 5*B*) and 1-amino-cyclopropyl carboxylic acid (ACPC; Fig. 5*C*) acting at wild-type and chimeric NMDARs. As we have observed in the case of glycine, replacement of the S1 region in the NR2A subunit with the corresponding region from NR2D has little effect on the potency of each of these NR1 agonists. In contrast to what we have observed with glycine, exchanging the S2 region of NR2A with that of NR2D also has little effect on the potency of D-serine and ACPC. Replacing the NR2A S2 region with the NR2D S2 region increases β-F-DL-alanine potency by ~9-fold, similar to glycine. Swapping both S1 and S2 domains leads to further increases in NR1 agonist potency for D-serine and ACPC; however, for β-F-DL-alanine its potency at the NR2A(2D-S1S2) chimera was similar to that seen at the NR2A(2D-S2) chimera. The extent of potency shifts are shown in Fig. 6.

Glycine potency is not influenced by the nature of the agonist acting at the NR2-ligand-binding site

In AMPARs, the efficacy of channel activation is correlated to the degree of domain closure of the LBD (Jin *et al.* 2003). Although it is unclear whether this is the case for agonist activation at the NR2-glutamate binding pocket, we examined whether using a partial agonist to activate the glutamate binding pocket rather than a full agonist such as glutamate would alter glycine potency. Supplemental Fig. 2 shows the effect of using the NR2A partial agonist, homoquinolinate (Erreger *et al.* 2005*b*; 30 μM) rather than glutamate to activate the NMDAR constructs. Glycine potencies with homoquinolinate were similar to those obtained when glutamate was used as the agonist for NR1/NR2A and NR1/NR2D receptors. Glycine concentration–response curves had EC_{50} values of $1.91 \pm 0.14\,\mu$M ($n = 9$) for NR1/NR2A, 194 ± 14 nM ($n = 6$) for NR1/NR2D(WT), and 136 ± 7 nM ($n = 14$) for NR1/NR2A(2D-S1S2). Thus using a partial agonist

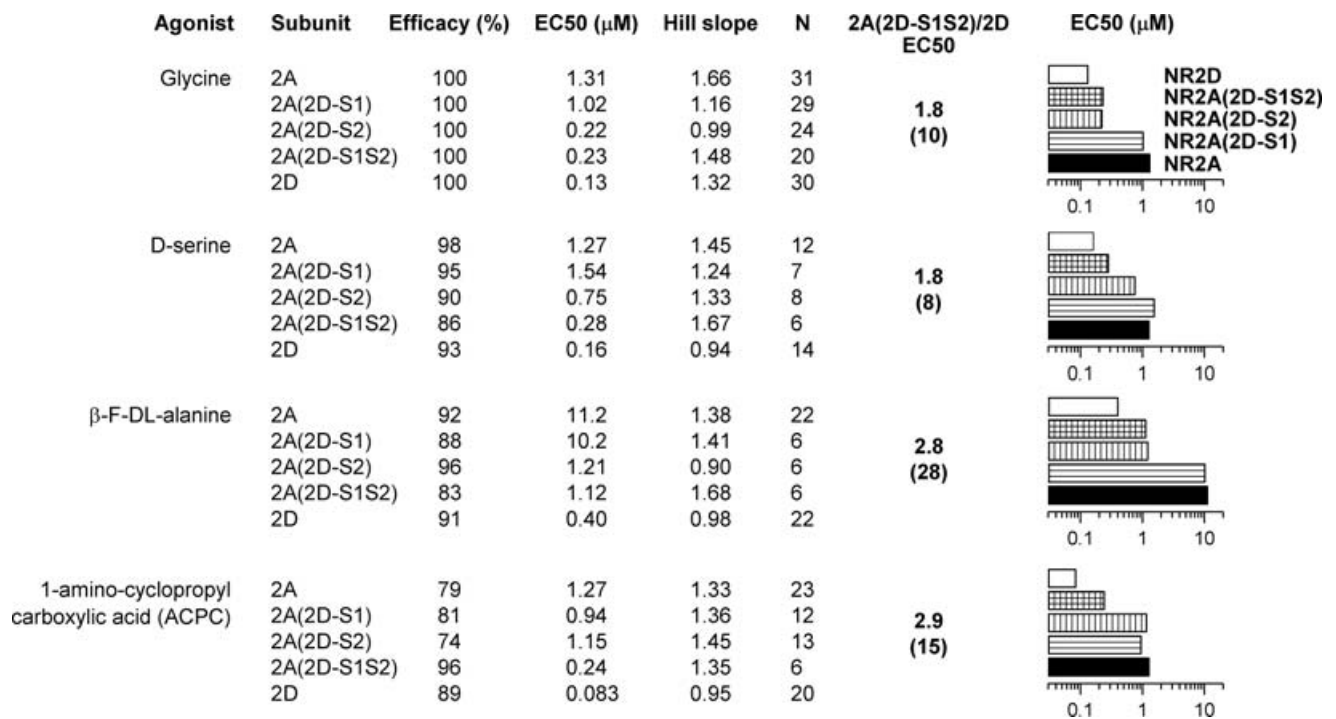| Agonist	Subunit	Efficacy (%)	EC50 (μM)	Hill slope	N	2A(2D-S1S2)/2D EC50	EC50 (μM)
Glycine	2A	100	1.31	1.66	31		
	2A(2D-S1)	100	1.02	1.16	29		
	2A(2D-S2)	100	0.22	0.99	24	1.8 (10)	
	2A(2D-S1S2)	100	0.23	1.48	20		
	2D	100	0.13	1.32	30		
D-serine	2A	98	1.27	1.45	12		
	2A(2D-S1)	95	1.54	1.24	7		
	2A(2D-S2)	90	0.75	1.33	8	1.8 (8)	
	2A(2D-S1S2)	86	0.28	1.67	6		
	2D	93	0.16	0.94	14		
β-F-DL-alanine	2A	92	11.2	1.38	22		
	2A(2D-S1)	88	10.2	1.41	6		
	2A(2D-S2)	96	1.21	0.90	6	2.8 (28)	
	2A(2D-S1S2)	83	1.12	1.68	6		
	2D	91	0.40	0.98	22		
1-amino-cyclopropyl carboxylic acid (ACPC)	2A	79	1.27	1.33	23		
	2A(2D-S1)	81	0.94	1.36	12		
	2A(2D-S2)	74	1.15	1.45	13	2.9 (15)	
	2A(2D-S1S2)	96	0.24	1.35	6		
	2D	89	0.083	0.95	20		

Figure 6. Summary of the pharmacological properties and 'relative efficacies' of ligands acting at the NR1 coagonist binding site for wild-type and chimeric NMDARs

Mean EC_{50} and Hill slope values obtained from fitting concentration–response relationships for a series of NR1 agonists acting at wild-type and chimeric NMDARs. Efficacy denotes the maximal current response to the test agonist relative to the maximal response to glycine. The ratio of the EC_{50} at NR1/NR2A(2D-S1S2) compared to NR1/NR2D NMDARs is given to indicate the extent to which incorporation of the S1 and S2 regions from the NR2D NMDAR subunit results in a more 'NR2D-like' agonist potency. For comparison the ratio of EC_{50} at NR1/NR2A to NR1/NR2D NMDARs is indicated in parentheses. The dependence of the EC_{50} for each agonist at the various constructs is illustrated as bar graphs to the right of these ratios.

to activate NMDARs does not alter the glycine potency obtained when the corresponding receptor is activated by a full NR2 agonist.

Chimeric NR2A subunits containing NR2D M1, M2 and M3 membrane domains display no change in glycine potency

Macroscopic measurements such as the EC_{50} value of an agonist are determined by microscopic rate constants that describe both binding and gating reactions (see Colquhoun, 1998). NR2D-containing NMDARs have characteristically different biophysical properties compared to those containing NR2A subunits (Monyer *et al.* 1994; Wyllie *et al.* 1996, 1998; Vicini *et al.* 1998). For example, NR2D-containing NMDARs exhibit 'low-conductance' single-channel openings compared to the 'high-conductance' NR2A-containing receptors. In addition, the overall probability that a channel is open during an activation is considerably less for NR2D-containing NMDARs (Wyllie *et al.* 1998). The pore-forming regions of ligand-gated ion channels are likely to control/influence rate constants that describe 'gating' reactions. We therefore examined whether transferring the M1, M2 and M3 membrane associated domains of the NR2D subunit into NR2A-containing NMDARs similarly altered glycine potency. Supplemental Fig. 3 shows mean concentration–response curves for glutamate and glycine acting at NR2A(2D-M1M2M3) and NR2A(2D-S1M1M2M3S2) chimeras. When only the M1, M2 and M3 regions were transferred from NR2D into NR2A neither glutamate potency ($3.28 \pm 0.16 \, \mu$M, $n = 13$; Suppl. Fig. 3A) nor glycine potency ($1.36 \pm 0.10 \, \mu$M, $n = 9$; Suppl. Fig. 3B) were different from the corresponding values seen with NR2A(WT)-containing NMDARs. By contrast, increases in both glutamate and glycine potencies were observed when NR2D membrane associated domains as well as S1 and S2 regions were included in the chimeric construct (EC_{50}(glut) $= 429 \pm 24 \,$nM, $n = 8$; EC_{50}(gly) $= 311 \pm 17 \,$nM, $n = (11)$).

Potency of the glycine-site antagonist, 5,7-DCKA at wild-type and chimeric NMDARs

In addition to the actions of agonists at the NR1 coagonist binding site and the influence of NR2 S1 and S2 regions on their potencies we also considered whether the action of competitive antagonists could be affected by the nature of the NR2 subunit present in the heteromeric NMDAR complex. We examined the effect of 5,7-dichlorokynurenic acid (5,7-DCKA, Baron *et al.* 1990; McNamara *et al.* 1990) by measuring the concentration of antagonist required to inhibit responses by 50% for NR2A(WT)-,

NR2D(WT)-, NR2A(2D-S1)-, NR2A(2D-S2)- and NR2A(2D-S1S2)-containing NMDARs. In addition, we measured the equilibrium constant, K_B, by the Schild method for this antagonist at NR2A(WT)-, NR2D(WT)- and NR2A(2D-S1S2)-containing NMDARs.

Figure 7A shows a TEVC current recording obtained from an oocyte expressing NR1/NR2A NMDARs. Currents were evoked by a saturating concentration of glutamate (50 μM) and the EC_{50} concentration of glycine (1.5 μM) for this receptor combination. Increasing the concentration of 5,7-DCKA from 10 nM to 3 μM results in a concentration-dependent decrease in the magnitude of the current recorded. Figure 7B shows mean inhibition curves for this receptor and the others studied. As would be anticipated if glycine had different affinities for these two receptor subtypes, 5,7-DCKA is most potent at inhibiting responses mediated by NR1/NR2A NMDARs ($IC_{50} = 96 \pm 7 \,$nM, $n = 5$) and least potent when acting at NR1/NR2D NMDARs ($IC_{50} = 1.7 \pm 0.15 \, \mu$M, $n = 6$; glycine concentration $= 150 \,$nM). Chimeric NR2A receptor subunits showed intermediate IC_{50} values for 5,7-DCKA that were $226 \pm 46 \,$nM ($n = 12$; glycine concentration $= 1 \, \mu$M) for NR1/NR2A(2D-S1), $269 \pm 21 \,$nM ($n = 6$; glycine concentration $= 250 \,$nM) for NR1/NR2A(2D-S2), and $322 \pm 32 \,$nM ($n = 8$; glycine concentration $= 250 \,$nM) for NR1/NR2A(2D-S1S2).

IC_{50} values for antagonist action at NMDARs are dependent on the concentration and identity of the agonist used (for example see Frizelle *et al.* 2006; Wyllie & Chen, 2007). Thus, although we carried out our measurements of IC_{50} values using equipotent concentrations of glycine for each receptor combination examined, differences in rate constants governing binding and gating reactions may also influence the observed IC_{50}. In this regard, we also determined the affinity of 5,7-DCKA for its binding site in the NR1 subunit by performing Schild analysis to obtain K_B values for this antagonist acting at NR2A-, NR2D- and NR2A(2D-S1S2)-containing NMDARs. Supplemental Fig. 4 shows examples of two-point concentration–response curves, for each of these receptor combinations, generated in the absence and in the presence of increasing concentrations of 5,7-DCKA. The Schild plots obtained by pooling data from several such experiments are illustrated in Fig. 7C–E. The fitted lines in each case show the fit of the data points with the Schild equation and the intercept with the abscissa gives the K_B for 5,7-DCKA (see Methods). No significant differences were observed for any of the receptor combinations examined and the mean K_B values were $80 \pm 2 \,$nM for NR1/NR2A ($n = 6$; Fig. 7C), $70 \pm 3 \,$nM for NR1/NR2D ($n = 6$; Fig. 7D), and $79 \pm 4 \,$nM for NR2A(2D-S1S2) ($n = 5$; Fig. 7E). Indeed, the estimates of the K_B for 5,7-DCKA obtained in the present study are in good agreement with a previously published value obtained from Schild analysis of its antagonism

of NMDA receptor-mediated responses recorded from oocytes expressing whole-brain mRNA (McNamara *et al.* 1990) but indicate a higher affinity of 5,7-DCKA binding than has been reported for the NR1 S1S2 fusion protein (540 nM; Furukawa & Gouaux, 2003). These data suggest that 5,7-DCKA does not sense the same structural differences in the NR2 subunits that glycine does, which may reflect different degrees of domain closure induced by ligand binding to NR1 (Furukawa & Gouaux, 2003). This may also reflect predominant contact residues in the NR1

Domain1 (Furukawa & Gouaux, 2003), which is likely to be minimally influenced by structural changes in Domain2 for NR2D *versus* NR2A.

These data suggest that the identity of the NR2 subunit coexpressed with the NR1 subunit does not cause global structural changes within this binding site that lead to reduction in affinity of all ligands since antagonists are insensitive to the identity of the NR2 subunit present in the NMDAR complex. Rather, it seems likely that inter-actions between NR1 and NR2 subunits that occur after
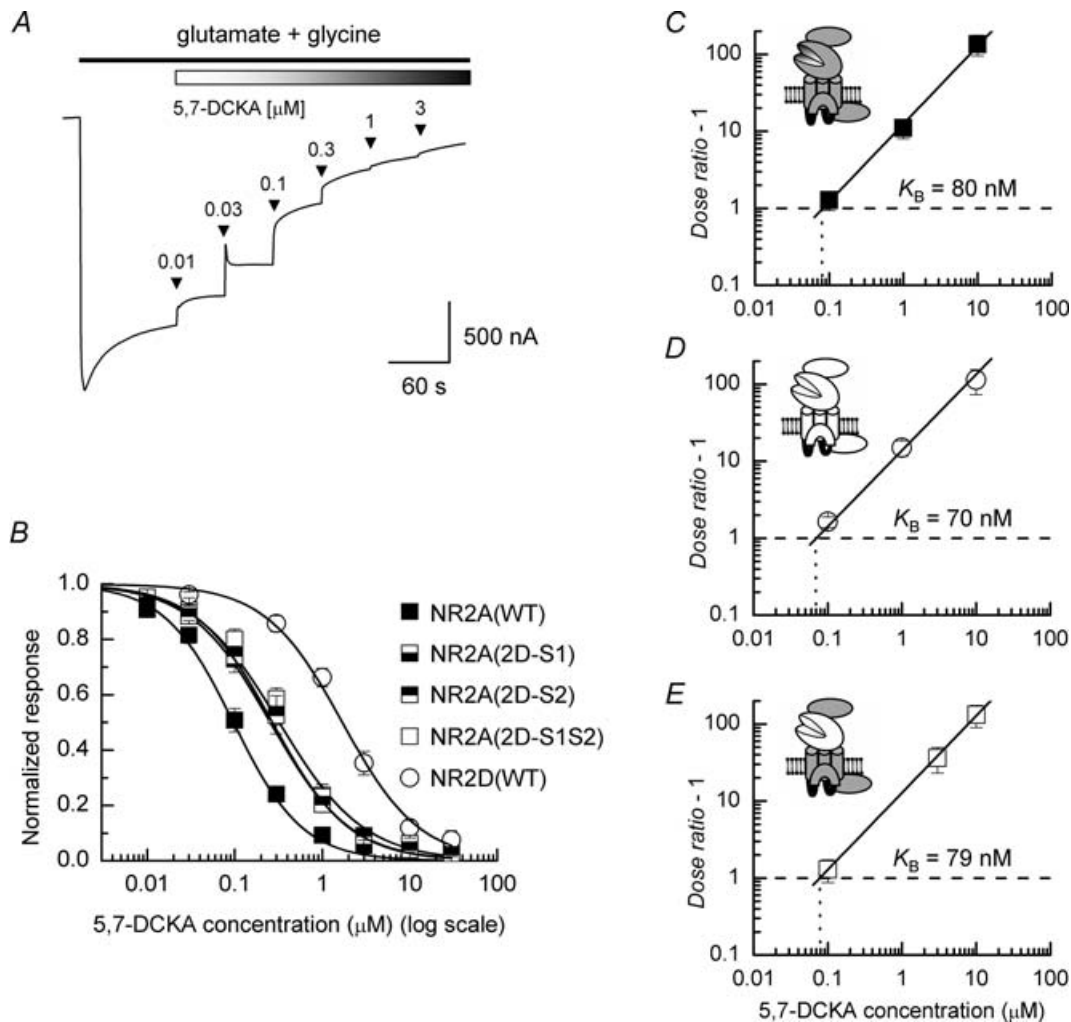
Figure 7. Antagonism of wild-type and chimeric NMDAR mediated responses by 5,7-DCKA
A, representative TEVC current recording of the inhibition by 5,7-DCKA of a NR1/NR2A(WT) NMDAR-mediated response. In this recording the glycine concentration was set to be equal to the EC_{50} concentration at this receptor combination (1.5 μM) whereas the glutamate concentration was set at a saturating level (50 μM). *B*, mean inhibition curves for 5,7-DCKA antagonism of responses mediated by NR1/NR2A(WT) and NR1/NR2D(WT) NMDARs and each of the three 'binding' domain chimeric NMDARs. *C–E*, Schild analysis of 5,7-DCKA antagonism. The mean dose ratios, *r*, measured from the parallel shifts of two-point concentration–response curves (Supplemental Fig. 4) are plotted on a log–log scale as (*r* – 1) *versus* antagonist concentration, [B]. If the slope of the linear regression fit of the data points was sufficiently close to 1 (as is to be expected of competitive antagonism), the data were refitted with the Schild equation (*r* – 1) = [B]/K_B, where the slope of the line is unity and the equilibrium constant for antagonist binding, K_B, is given by the intercept on the *x*-axis. Similar K_B values for 5,7-DCKA were obtained for NR2A(WT), NR2D(WT) and NR2A(2D-S1S2) NMDARs.

ligand binding and lead to channel opening are responsible for differences in the glycine-site agonist potency observed.

Comparison of NR2A and NR2D ligand-binding domains and identification of residues in NR2 subunits that influence glycine potency

In order to understand how the identity of the NR2 subunit influences glycine's actions at NR1, we evaluated

hydrated models of NR2A and NR2D using molecular dynamics (see Methods). Figure 8*A* shows the bi-lobar structure of the NR1/NR2A agonist binding domain dimer (grey). Superimposed on this is the equivalent structure of the NR1/NR2D agonist binding domain dimer (purple). Figure 8*B* shows a superimposition of the NR1 ligand binding sites (with glycine bound) at the end of a 10 ns simulation of the heterodimeric NR1–NR2A and NR1–NR2D dimer–dimer. These simulations demonstrate that glycine is predicted to
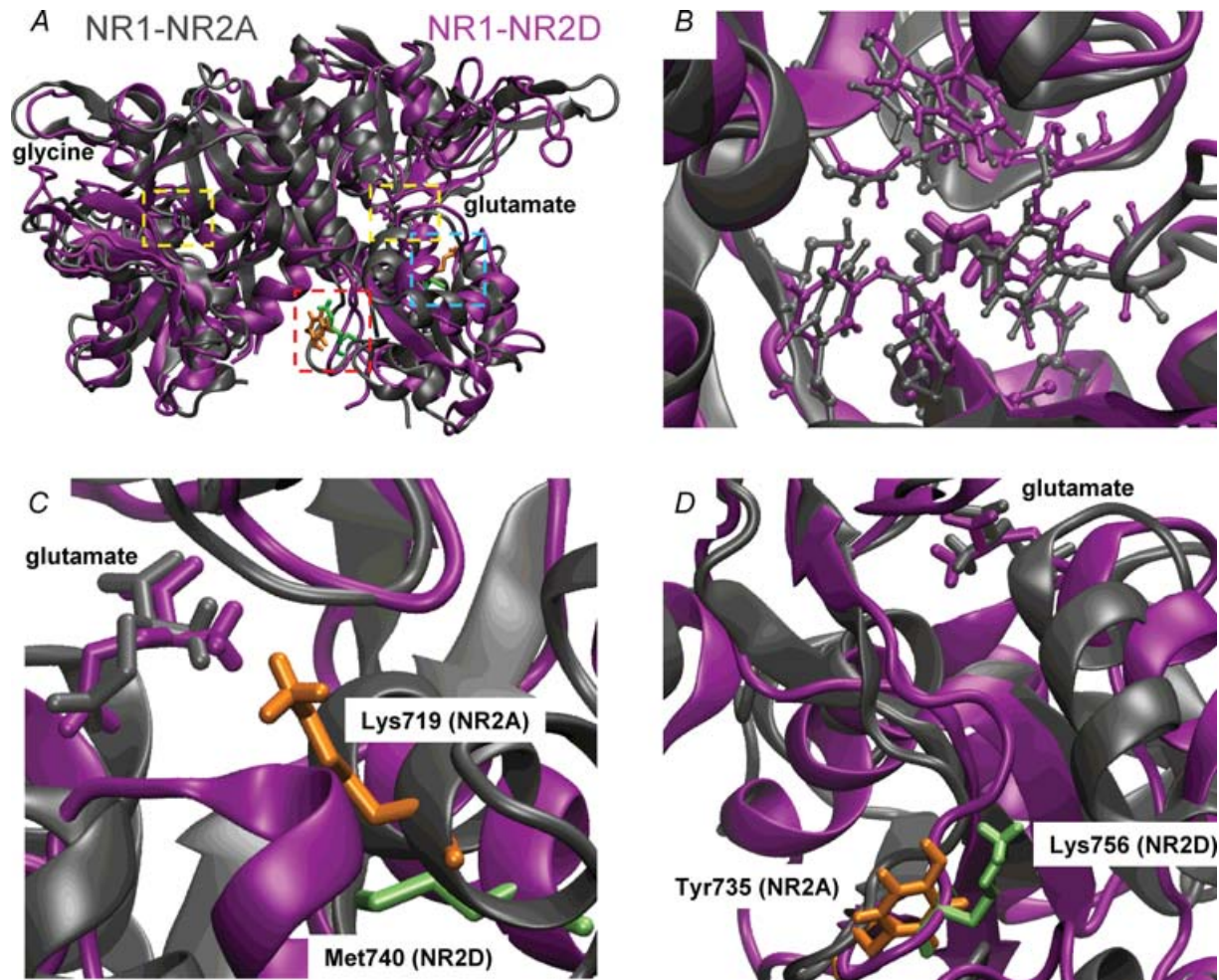
Figure 8. Comparison of NR1/NR2A and NR1/NR2D glycine binding pockets and identification of NR2 residues that influence glycine potency

A, superimposition of NR1/NR2A (grey) and NR1/NR2D (purple) agonist binding domain dimers. The locations of the glutamate and glycine binding sites are highlighted by the yellow dashed-line boxes, with the glycine binding site shown in greater detail in panel *B*. The blue and red dashed-line boxes highlight the regions in the NR2A and NR2D D2 domains that are shown in greater detail in *C* and *D*, respectively. *B*, expanded view of the NR1 glycine binding site when associated with NR2A (grey) or NR2D (purple) showing that despite different potencies, both protein backbone and sidechains of the glycine binding site are predicted to be quite similar after 10 ns of simulation. *C*, illustration of the locations of Lys719 (NR2A, orange) and Met740 (NR2D, light green) in Domain2 of each NR2 NMDAR subunit. These residues are distant from the NR1–NR2 interface (indicated by the blue dashed-line box in *A* seen from a different orientation). Likewise, the carboxylate group of glutamate (when it occupies its binding site) and Lys719 are separated by more than 10 Å. *D*, illustration of the locations of Tyr735 (NR2A, orange) and Lys756 (NR2D, green) in Domain2 of each NR2 NMDAR subunit, positioned in the lower interface between NR1 and NR2 (indicated by the red dashed-line box in *A* seen from a different orientation).

adopt a very similar orientation in the NR1/NR2A and NR1/NR2D glycine binding pockets, even though differences develop in the positions of amino acid residues that interact directly with glutamate in each of these NR2 NMDAR subunits (see Erreger *et al.* 2007). However, these differences in the positioning of amino acids in the NR2 binding pocket *per se* are unlikely to account for NR2–NR1 interactions that ultimately lead to differences in glycine potencies seen at NR1/NR2A and NR1/NR2D NMDARs. Rather, the simulations suggest that the differences in Domain2 of the NR2 are well positioned to influence NR1 function.

Inspection of the sequence throughout the S2 region (Fig. 1*B*; Suppl. Fig. 1) in NR2A and NR2D subunits that encodes most of Domain2 reveals several differences in amino acid sequence. Moreover, as glycine potency is also greater at NR2B- and NR2C-containing NMDARs than in NR2A-containing NMDARs, we examined whether these amino acid differences were also observed between NR2A and these two other NMDAR subunits. There are two residues within the S2 region that are conserved in NR2B, NR2C and NR2D subunits but are different in the NR2A subunit and which result in charged/uncharged residue exchanges in these subunits. These are Lys719 in NR2A (equivalent to Met740 in NR2D) and Tyr735 in NR2A (equivalent to Lys756 in NR2D). The positions of each of these sites are highlighted in Fig. 1*B* and Suppl. Fig. 1. Figure 8*C* and *D* shows the location of each of these residues in our superimposed hydrated models of NR1/NR2A and NR1/NR2D agonist binding domain dimers. As discussed below, at least one of these NR2 residues appears to mediate with the NR1 subunit and may contribute, in part, to the differences in glycine potency seen at various NMDARs.

We created point mutations in the NR2A subunit to generate sequences that contained the NR2D subunit residue to determine whether either of these residues was responsible for the difference in glycine potency at NR2A- and NR2D-containing NMDARs. Figure 9*A* shows the NR1/NR2A agonist binding domain dimer with the location of Tyr735 in NR2A indicated along with the locations of glycine and glutamate in their respective binding sites. In Fig. 9*B*, a higher resolution image illustrates how Tyr735 in the NR2A subunit is predicted to form a hydrogen-bonding network with Glu786 and Lys790 in the NR1 subunit as well as Tyr679 in NR2A. A representative TEVC current trace showing responses to increasing concentrations of glycine and obtained from an oocyte expressing NR1/NR2A(K719M Y735K) NMDARs is illustrated in Fig. 9*C*. Figure 9*D* shows mean glycine concentration–response curves for the NR2A(K719M) and NR2A(Y735K) mutations (mimicking the residues found in NR2D subunits). Each of these mutations resulted in an increase in glycine potency with EC_{50} values for glycine of 231 ± 10 nM ($n = 33$)

and 362 ± 18 nM ($n = 12$) for NR2A(K719M) and NR2A(Y735K), respectively. However, the introduction of the two point mutations into the NR2A subunit, NR2A(K719M Y735K), did not result in a further increase in glycine potency and gave a mean EC_{50} value of 277 ± 7 nM ($n = 12$). In addition, replacing the lysine residue at position 719 in NR2A with a glutamate residue (K719E) to alter the charge at this position also gave rise to an NMDAR with increased glycine potency (Suppl. Fig. 5*A*). Each of these point mutations also caused, albeit smaller, shifts in glutamate potency (Suppl. Fig. 5*B* and *C*). We therefore presume that while the NR2A Met719 and Lys735 mutant residues are important for modulating glycine potency, the wild-type sequence of the subunit is also critical for the overall effect.

We also examined the effects of introducing the residues present in NR2A subunits into the NR2D subunit. Figure 10*A* shows the NR1/NR2D agonist binding domain dimer with the location of Lys756 in NR2D indicated. The positions of glycine and glutamate in their respective binding sites are also indicated. Figure 10*B* shows the predicted interaction of Lys756, in the NR2D subunit with Glu786 in NR1. Unlike Tyr735 in NR2A, the NR2D residue Lys756 develops a different set of interactions with Glu786 in NR1 and Val757 in NR2D while no interaction with the side-chain of the Lys790 residue in NR1 is predicted as seen in Fig. 9*B*. This change in the hydrogen-bonding network at the interface between domains may correlate with the effect on glycine potency. Figure 10*C* shows an example of a TEVC current trace illustrating the increase in the response to cumulative applications of increasing concentrations of glycine, obtained from an oocyte expressing NR1/NR2D(K756Y). The initial response shows the effect of perfusing the oocyte with a solution containing only glutamate (no added glycine) and allows us to estimate the levels of 'contaminating' glycine in our solutions (Johnson & Ascher, 1992; Traynelis *et al.* 1995). We estimated the level of this contamination to be < 10 nM (6.7 ± 1 nM; $n = 9$). As can be seen from this example TEVC current trace and the mean concentration–response curves (Fig. 10*D*), the NR2D(K756Y) point mutation increases the sensitivity of the receptor to glycine. The (uncorrected) mean EC_{50} value for this construct is 26 ± 1 nM ($n = 21$) suggesting a 'true' EC_{50} of around 20 nM. Mutation of Met740 to a lysine residue, NR2D(M740K), however, did not result in any change in glycine potency when compared to NR2D(WT)-containing NMDARs ($EC_{50} = 149 \pm 7$ nM, $n = 20$; Fig. 10*D*). The glutamate sensitivity of NR2D(M740K)-containing NMDARs was not different from NR2D(WT) though a slight increase in glutamate potency is observed with the NR2D(K756Y) mutation (Suppl. Fig. 5*D*).

Thus, both our molecular modelling and mutagenesis studies would seem to suggest that these different

intersubunit contacts may provide qualitatively different associative interactions between the D2 domains of NR1 and NR2A than between NR1 and NR2D, a potential basis of why differences in glycine potencies exist in various NR1/NR2 NMDARs.

Discussion

The most important result of this work is the identification of Domain2 of the NR2 subunit as a molecular determinant of glycine potency. These data complement previous studies that have established that amino acid residues located in Domain 1 and 2 on the NR2 subunits contribute to the glutamate-binding pocket of NMDARs

(see Chen & Wyllie, 2006; Mayer, 2006). Furthermore, these findings help provide new information on how the variation in agonist potencies is observed among different recombinant NMDAR subtypes. Specific residues within Domain2 are highlighted as critical mediators of long-range intraprotein interactions that control glycine potency.

Structural interactions from the NR2D-S2 domain can influence glycine potency in recombinant NMDARs

Several studies have examined the differences in amino acid sequence between NR2 subunits in order to identify NMDAR subtype specific ligands (Feng *et al.* 2004;
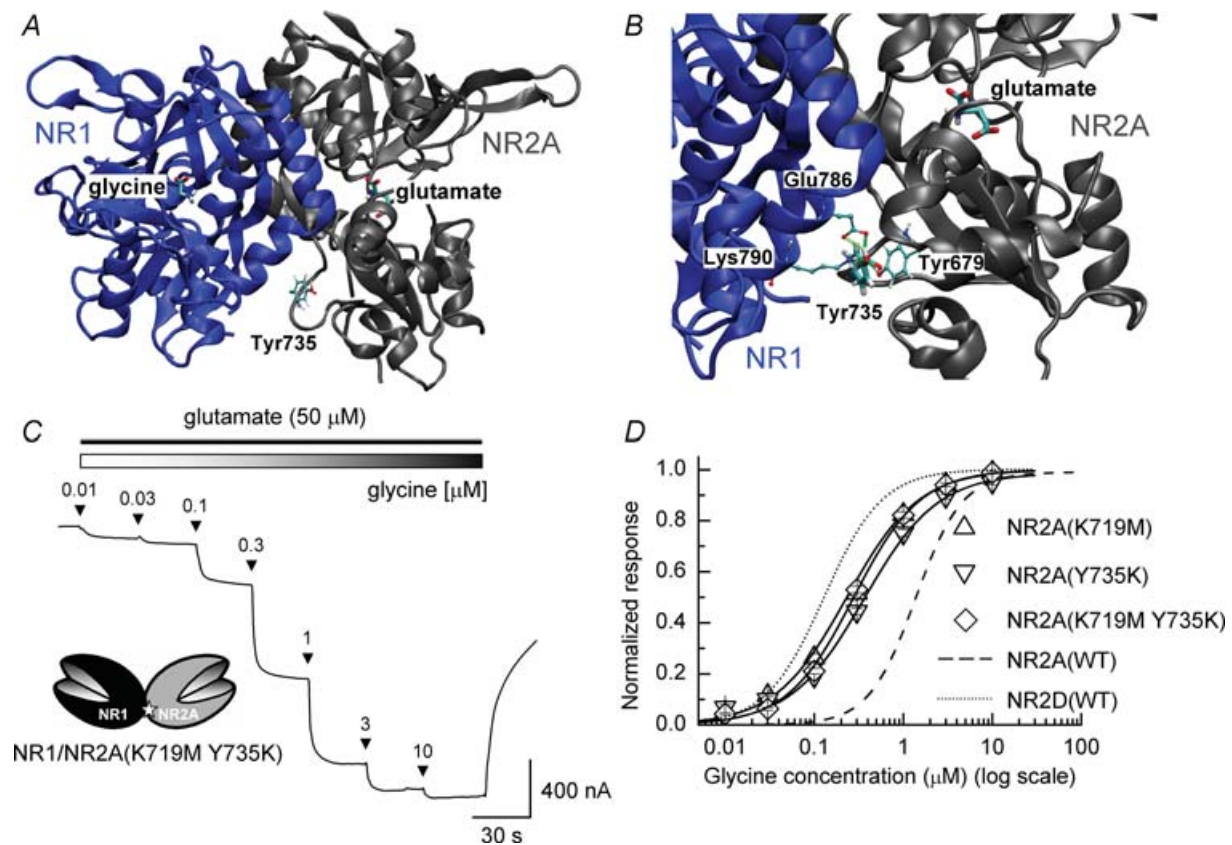

Figure 9. Analysis of the effects of point mutations in the S2 region of the NR2A subunit on glycine potency

A, view of the NR1/NR2A agonist binding domain dimer. The positions of glycine and glutamate in their respective binding sites are indicated, together with the Tyr735 residue located in Domain2 of NR2A. *B,* a frame from the MD simulation of NR1/NR2A agonist binding domain dimer showing the hydrogen–bond interactions of Tyr735 in the NR2A subunit with residues Glu786 and Lys790 in the NR1 subunit and Tyr679 of NR2A. The location of glutamate in its binding site is also indicated. *C,* example TEVC current trace obtained in responses to applications of increasing concentrations of glycine (0.01–10 μM) and recorded from an oocyte expressing NR1/NR2A(K791M Y735K) NMDARs. *D,* mean glycine concentration–response curves for NR1/NR2A(K719M), NR1/NR2A(Y735K) and NR1/NR2A(K719M Y735K) NMDARs. Each of the point mutations result in a shift to the left in glycine potency to values that are similar to those seen for NR2D(WT)-containing NMDARs. Mean Hill slopes and mean maximal currents recorded were for NR2A(K719M): 1.08 ± 0.02, 1.9 ± 0.1 μA; for NR2A(Y735K): 1.05 ± 0.04, 3.0 ± 0.2 μA; and for NR2A(K719M Y735K): 1.16 ± 0.02, 3.8 ± 0.3 μA. The dashed and dotted lines show the corresponding glycine concentration–response curve for NR2A(WT)- and NR2D(WT)-containing NMDARs, respectively.

Kinarsky *et al.* 2005; Erreger *et al.* 2007). Other studies have shown that specific residues that contact ligand in crystal structures control glutamate and glycine potency in functional receptors (Kuryatov *et al.* 1994; Laube *et al.* 1997; Anson *et al.* 1998, 2000; Chen *et al.* 2004, 2005; Erreger *et al.* 2007). Interestingly, mutations of residues that contact glutamate within the NR2 LBD and reduce glutamate potency have little effect on glycine potency (Anson *et al.* 1998; Chen *et al.* 2005; for review see Chen & Wyllie, 2006), suggesting that the effects of the NR2 sub-unit on glycine potency are unlikely to involve differences in glutamate binding. Similarly, point mutations within the NR1 glycine binding pocket that alter glycine potency have little effect on glutamate potency (Kuryatov *et al.*

1994; Wafford *et al.* 1995; Williams *et al.* 1996). Thus, impaired binding within one subunit does not seem to greatly influence potency of agonist binding to the other subunit. This is supported by our observation that using either a full or partial agonist to activate the NR2-glutamate binding site has little influence on glycine potency. This raises the idea that other features of the agonist binding domains or their function must, respectively, influence agonist potency.

Evidence has shown that in terms of agonist efficacy both NR1 and NR2 agonist binding pockets may rely on distinct mechanisms (Furukawa & Gouaux, 2003; Erreger *et al.* 2005*b*; reviewed in Kristensen *et al.* 2006). For example, in contrast to the correlation between domain closure
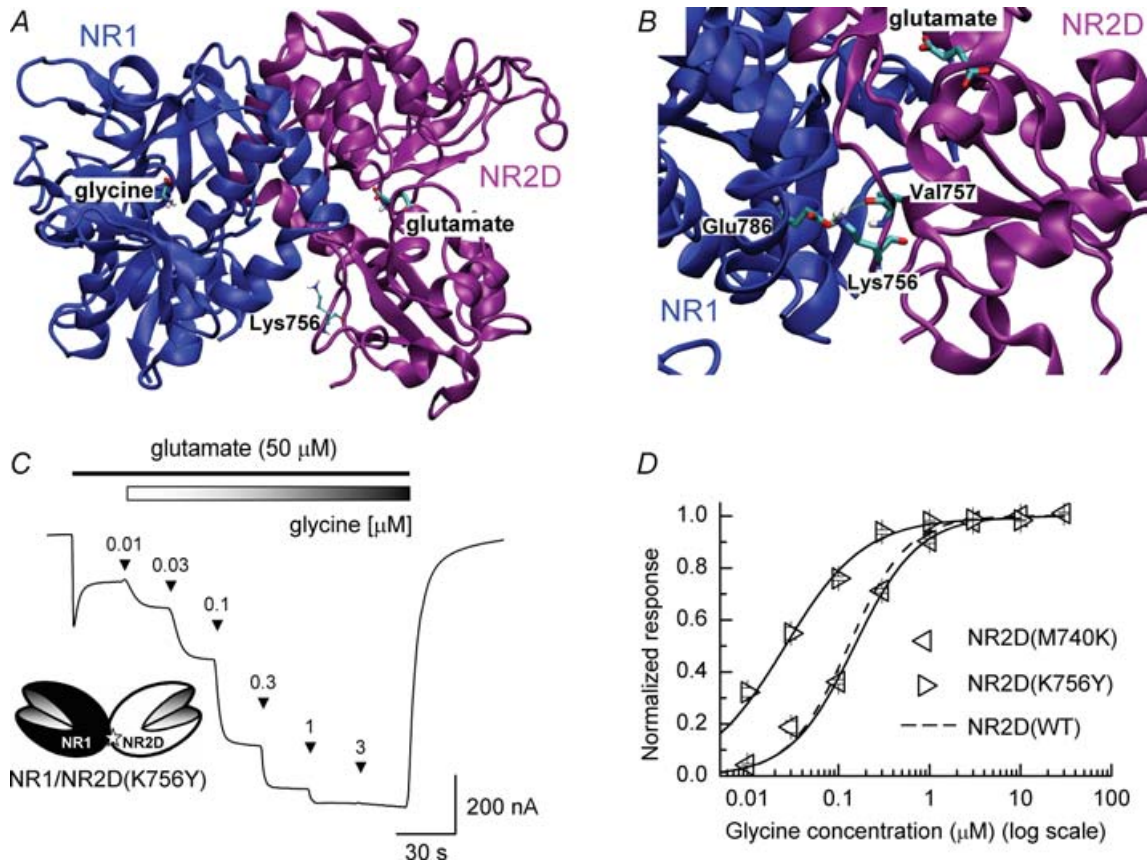

Figure 10. Analysis of the effects of point mutations in the S2 region of the NR2D subunit on glycine potency
A, view of the NR1/NR2D agonist binding domain dimer The positions of glycine and glutamate in their respective binding sites are indicated, together with the Lys756 residue located in Domain2 of NR2D. *B*, a frame from the MD simulation of NR1/NR2D agonist binding domain dimer showing the hydrogen bonding between Lys756 in the NR2D subunit and residues Glu786 in the NR1 subunit and Val757 of NR2D. The location of glutamate in its binding site is also indicated. *C*, example TEVC current trace obtained in responses to applications of increasing concentrations of glycine (0.01–3 μM) and recorded from an oocyte expressing NR1/NR2D(K756Y) NMDARs. Note that the initial response is obtained in the presence of no added glycine. Such recordings were used to estimate the levels of 'contaminating' glycine in our recording solutions. *D*, mean glycine concentration–response curve for NR1/NR2D(M740K) and NR1/NR2D(K756Y) NMDARs. The NR2D(M740K) mutation causes no change in glycine potency compared to NR2D(WT). Mean Hill slopes and mean maximal currents recorded for NR2D(M740K): 1.23 ± 0.06, 0.35 ± 0.15 μA. In contrast the NR2D(K756Y) mutation resulted in an increase in glycine potency. Mean Hill slopes and mean maximal currents recorded for NR2D(K756Y): 0.99 ± 0.04, 0.48 ± 0.09 μA. The dashed line shows the corresponding glycine concentration–response curve for NR2D(WT)-containing NMDARs.

and agonist efficacy for the GluR2 and GluR5/6 pockets (Jin *et al.* 2003; Mayer, 2005; Nanao *et al.* 2005), partial and full agonists for the NR1-glycine binding pocket induce the same degree of domain closure (Inanobe *et al.* 2005). It is still unclear whether there is a correlation between agonist efficacy and the degree of domain closure for the NR2-glutamate binding pocket. However, the insertion of steric clashes within the NR2B-glutamate pocket has suggested that the domain closure may be correlated with agonist efficacy for certain agonists (Hansen *et al.* 2005).

Our results suggest that the influence of the NR2D-S2 region on glycine potency is mediated by interactions between the glutamate and glycine LBDs from the NR1 and NR2 subunits. Because NMDARs containing chimeras with either the NR2D S1 or S2 regions showed increased glutamate potency but only the NR2A(2D-S2) chimera influenced glycine potency, modification of glutamate potency (in either direction) seems unlikely to be the predominant cause of changes in glycine potency. These data suggest that interactions either directly or indirectly induced by the conformational arrangement of the NR2-S2 domain with the other subunits are able to sway the receptor's sensitivity to glycine. Consistent with this idea, the S2 region of the NR2 subunit shows the largest predicted divergence in structure in molecular dynamics simulations of NR1/NR2A and NR1/NR2D (Erreger *et al.* 2007).

Interestingly, the insertion of the NR2D-S2 sequence into NR2A does not change the affinity of a competitive antagonist at the NR1-glycine binding pocket, suggesting that the contact residues have not undergone any significant structural changes. This idea is supported by our molecular dynamics simulations, which predict little difference between the NR1/NR2A and NR1/NR2D glycine binding sites. In further support of this idea is the fact that we observed shifts in potencies at chimeric NMDARs with D-serine, β-F-DL-alanine and ACPC when they were used as NR1 agonists. As each of these agonists will adopt different conformations within the NR1 LBD and interact with different contact residues it would seem unlikely that structural changes in the NR2 subunit would give rise to changes at the NR1 binding pocket that result in the changes in potency we have observed. Thus, we conclude that cross-subunit effects must be occurring downstream of the initial binding event at the pocket, perhaps being mediated by conformational changes in the protein as it translates the ligand binding event into the opening of the ion pore. Our data show that the NR2D ion pore itself has little influence on the changes in glycine potency we have observed (i.e. M1–M3; Suppl. Fig. 3), suggesting that the LBD and the ion pore functional domains act independently in this respect. The crystal structure of the NR1/NR2A LBD heterodimer has suggested that like the non-NMDAR GluR2 S1S2 homodimer, a number of interpocket interactions exist (Furukawa *et al.* 2005) and that these

may have functional consequences on receptor function. Furukawa *et al.* (2005) observed that the conformation of S2 domains showed the greatest dissimilarities upon superimposition of the NMDAR and non-NMDAR binding pockets. These data are consistent with our molecular dynamics analysis. Thus the regions of the LBDs encoded by the S2 region may adopt a structural conformation unique to NMDARs that may influence the interaction between the glycine and glutamate binding pockets. The identification of two specific residues in different parts of Domain2 of NR2 subunits that affect glycine potency indicates a complex interaction between the Domain2 of NR2 and NR1. One of these residues (Tyr735 (in NR2A), Lys756 (in NR2D); Figs 9 and 10) is at the interface between Domain2 of NR1 and Domain2 of NR2 and could play a role in the equilibrium of that interface or in interacting with linker regions during a gating event. Moreover, linker regions connecting the LBD to the transmembrane regions are not represented in crystal structures, but are encoded by S1 and S2 regions of the cDNA, and seem likely candidates for influencing the ability of agonist binding to open the permeation pore. Our results, however, indicate that the introduction of the corresponding NR2A residues into the NR2D subunit did not decrease glycine potency. Indeed, in the case of the NR2D(K756Y) mutation we generated an NMDAR with a lower EC_{50} for glycine than that seen with NR2D(WT)-containing NMDARs. The reasons for this increase in glycine potency are unclear, but it suggests that converting NR2D-containing NMDARs to receptors with lower sensitivities to glycine is likely to involve other, as yet unidentified regions of the NR2D subunit.

The contribution of interlobe atomic interactions to glutamate potency has recently become relevant for non-NMDARs (Robert *et al.* 2005; Weston *et al.* 2006) and in NMDARs (Maier *et al.* 2007; Erreger *et al.* 2007). Even though the NR1–NR2A cocrystal structure is now available (Furukawa *et al.* 2005), little is known about the importance of interpocket interactions for agonist potency. Coupling occurs between the glutamate and glycine binding pockets in NMDARs (Vyklicky *et al.* 1990; Benveniste *et al.* 1990; Benveniste & Mayer, 1991; Kemp & Priestley, 1991; Lester *et al.* 1993; Priestley & Kemp, 1994) and part of the S1 region of the NR2A subunit has been suggested to influence glycine-dependent desensitization (Regalado *et al.* 2001). However, the relationship between the two pockets in influencing agonist potency has not been examined in great detail.

Heterogeneity of glycine potencies among different NMDAR subtypes

It is unclear whether differences in agonist potency influence physiological and pathophysiological mechanisms in neurons. Nevertheless, one would predict receptors at which glutamate and glycine have high affinity may be candidates for detecting trophic

effects of glutamate. This could be consistent with the early developmental expression of NR2D. Receptors with higher affinities for glutamate might also be more optimal for detecting spillover glutamate from the cleft or glutamate release by glial cells, which can reach concentrations of only a few micromolar (Lee *et al.* 2007). Similarly, receptors at which glutamate has lower affinity would mean that their activation would be more dependent on the high concentrations of glutamate released at synaptic sites. Indeed, in this respect, receptors with the highest sensitivity to glutamate (NR2D-containing NMDARs) have, as yet, not been found at synaptic locations. Although concentrations of glycine within the cerebrospinal fluid have been estimated at micromolar levels that would saturate the glycine site, the actual concentration of glycine in the synaptic cleft remains unknown. Saturation of the glycine site may be synapse dependent, influenced not only by NR2 subunit expression but also by the activity of local glycine transporters. The concentrations of other endogenous amino acids that are high affinity agonists at the glycine site, such as D-serine, will also have an impact on this question (Thomson *et al.* 1989; Supplisson & Bergman, 1997; Berger *et al.* 1998; Bergeron *et al.* 1998). Thus, the NR2 receptor control of glycine potency needs to be considered in circumstances where the glycine concentration is low. Indeed receptors displaying lower sensitivity to glycine are likely to be those targeted by glycine transport inhibitors.

Conclusion

NMDARs are unusual in that they require two different ligands to occupy unique binding sites within the receptor–channel. The basis of why glycine potency varies at different NMDAR subtypes is less clear when each of these contains the same glycine-binding (NR1) subunit. We have identified residues within Domain2 of the NR2 subunit that influence glycine potency and, in part, account for the heterogeneity in glycine potencies. Protein–protein interactions at the interfaces of non-NMDAR subunits control desensitization and deactivation and it is clear from our data that such interactions between NR1 and NR2 subunits are key to regulating receptor function. Together with our accompanying paper (Wrighton *et al.* 2008) these studies demonstrate that the LBD and its interaction with other functional domains influences two defining characteristics of this receptor family, namely glycine (coagonist) potency and voltage-dependent Mg^{2+} block.

References

Anson LC, Chen PE, Wyllie DJA, Colquhoun D & Schoepfer R (1998). Identification of amino acid residues of the NR2A subunit that control glutamate potency in recombinant NR1/NR2A NMDA receptors. *J Neurosci* **18**, 581–589.

Anson LC, Schoepfer R, Colquhoun D & Wyllie DJA (2000). Single-channel analysis of an NMDA receptor possessing a mutation in the region of the glutamate binding site. *J Physiol* **527**, 225–237.

Arunlakshana O & Schild HO (1959). Some quantitative uses of drug antagonists. *Br J Pharmacol Chemother* **14**, 48–57.

Banke TG & Traynelis SF (2003). Activation of NR1/NR2B NMDA receptors. *Nat Neurosci* **6**, 144–152.

Baron BM, Harrison BL, Miller FP, McDonald IA, Salituro FG, Schmidt CJ, Sorensen SM, White HS & Palfreyman MG (1990). Activity of 5,7-dichlorokynurenic acid, a potent antagonist at the N-methyl-D-aspartate receptor-associated glycine binding site. *Mol Pharmacol* **38**, 554–561.

Benveniste M, Clements J, Vyklicky L Jr & Mayer ML (1990). A kinetic analysis of the modulation of *N*-methyl-D-aspartic acid receptors by glycine in mouse cultured hippocampal neurones. *J Physiol* **428**, 333–357.

Benveniste M & Mayer ML (1991). Kinetic analysis of antagonist action at N-methyl-D-aspartic acid receptors. Two binding sites each for glutamate and glycine. *Biophys J* **59**, 560–573.

Berger AJ, Dieudonne S & Ascher P (1998). Glycine uptake governs glycine site occupancy at NMDA receptors of excitatory synapses. *J Neurophysiol* **80**, 3336–3340.

Bergeron R, Meyer TM, Coyle JT & Greene RW (1998). Modulation of N-methyl-D-aspartate receptor function by glycine transport. *Proc Natl Acad Sci U S A* **95**, 15730–15734.

Chen PE, Geballe MT, Stansfeld PJ, Johnston AR, Yuan H, Jacob AL, Snyder JP, Traynelis SF & Wyllie DJA (2005). Structural features of the glutamate binding site in recombinant NR1/NR2A *N*-methyl-D-aspartate receptors determined by site-directed mutagenesis and molecular modeling. *Mol Pharmacol* **67**, 1470–1484.

Chen PE, Johnston AR, Mok MH, Schoepfer R & Wyllie DJA (2004). Influence of a threonine residue in the S2 ligand binding domain in determining agonist potency and deactivation rate of recombinant NR1/NR2D NMDA receptors. *J Physiol* **558**, 45–58.

Chen PE & Wyllie DJA (2006). Pharmacological insights obtained from structure-function studies of ionotropic glutamate receptors. *Br J Pharmacol* **147**, 839–853.

Colquhoun D (1998). Binding, gating, affinity and efficacy: The interpretation of structure-activity relationships for agonists and of the effects of mutating receptors. *Br J Pharmacol* **125**, 924–947.

Cull-Candy SG, Brickley S & Farrant M (2001). NMDA receptor subunits: diversity, development and disease. *Curr Opin Neurobiol* **11**, 327–335.

Dingledine R, Borges K, Bowie D & Traynelis SF (1999). The glutamate receptor ion channels. *Pharmacol Rev* **51**, 7–61.

Erreger K, Chen PE, Wyllie DJA & Traynelis SF (2004). Glutamate receptor gating. *Crit Rev Neurobiol* **16**, 187–224.

Erreger K, Dravid SM, Banke TG, Wyllie DJA & Traynelis SF (2005*a*). Subunit specific gating controls rat recombinant NR1/NR2A and NR1/NR2B channel kinetics and synaptic signalling profiles. *J Physiol* **563**, 345–358.

Erreger K, Geballe MT, Dravid SM, Snyder JP, Wyllie DJA & Traynelis SF (2005*b*). Mechanism of partial agonism at NMDA receptors for a conformationally restricted glutamate analog. *J Neurosci* **25**, 7858–7866.

Erreger K, Geballe MT, Kristensen A, Chen PE, Hansen KB, Lee CJ, Yuan H, Le P, Lyuboslavsky PN, Micale N, Jørgensen L, Clausen RP, Wyllie DJA, Snyder JP & Traynelis SF (2007). Subunit-specific agonist activity at NR2A, NR2B, NR2C, and NR2D containing N-methyl-D-aspartate glutamate receptors. *Mol Pharmacol* **72**, 907–920.

Feng B, Tse HW, Skifter DA, Morley R, Jane DE & Monaghan DT (2004). Structure-activity analysis of a novel NR2C/NR2D-preferring NMDA receptor antagonist, 1-(phenanthrene-2-carbonyl)piperazine-2,3-dicarboxylic acid. *Br J Pharmacol* **141**, 508–516.

Frizelle PA, Chen PE & Wyllie DJA (2006). Equilibrium constants for (*R*)-[(*S*)-1-(4-bromo-phenyl)-ethylamino]-(2,3-dioxo-1,2,3,4-tetrahydroquinoxalin-5-yl)-methyl]-phosphonic acid (NVP-AAM077) acting at recombinant NR1/NR2A and NR1/NR2B NMDA receptors: implications for studies of synaptic transmission. *Mol Pharmacol* **70**, 1022–1032.

Furukawa H & Gouaux E (2003). Mechanisms of activation, inhibition and specificity, crystal structures of the NMDA receptor NR1 ligand-binding core. *EMBO J* **22**, 2873–2885.

Furukawa H, Singh SK, Mancussco R & Gouaux E (2005). Subunit arrangement of and function in NMDA receptors. *Nature* **438**, 185–192.

Gibb AJ (2006). Glutamate unbinding reveals new insights into NMDA receptor activation. *J Physiol* **574**, 329.

Hansen KB, Clausen RP, Bjerrum EJ, Bechmann C, Greenwood JR, Christensen C, Kristensen JL, Egebjerg J & Bräuner-Osbourne H (2005). Tweaking agonist efficacy at *N*-methyl-D-asparate receptors by site-directed mutagenesis. *Mol Pharmacol* **68**, 1510–1523.

Hollmann M, Boulter J, Maron C, Beasley L, Sullivan J, Pecht G & Heinemann S (1993). Zinc potentiates agonist-induced currents at certain splice variants of the NMDA receptor. *Neuron* **10**, 943–954.

Humphrey W, Dalke A & Schulten K (1996). VMD – Visual Molecular Dynamics. *J Mol Graphics* **14**, 33–38.

Ikeda K, Nagasawa M, Mori H, Araki K, Sakimura K, Watanabe M, Inoue Y & Mishina M (1992). Cloning and expression of the ε4 subunit of the NMDA receptor channel. *FEBS Lett* **313**, 34–38.

Inanobe A, Furukawa H & Gouaux E (2005). Mechanism of partial agonist action at the NR1 subunit of NMDA receptors. *Neuron* **47**, 71–84.

Jin R, Banke TG, Mayer ML, Traynelis SF & Gouaux E (2003). Structural basis for partial agonist action at ionotropic glutamate receptors. *Nat Neurosci* **6**, 803–810.

Johnson JW & Ascher P (1987). Glycine potentiates the NMDA response in cultured mouse brain neurons. *Nature* **325**, 529–531.

Johnson JW & Ascher P (1992). Equilibrium and kinetic study of glycine action on the *N*-methyl-D-aspartate receptor in cultured mouse brain neurons. *J Physiol* **455**, 339–365.

Kaminski GA, Friesner RA, Tirado-Rives J & Jorgensen WL (2001). Evaluation and reparametrization of the OPLS-AA force field for proteins via comparison with accurate quantum chemical calculations on peptides. *J Phys Chem B* **105**, 6474–6487.

Kemp JA & Priestley T (1991). Effects of (+)-HA-966 and 7-chlorokynurenic acid on the kinetics of *N*-methyl-D-aspartate receptor agonist responses in rat cultured cortical neurons. *Mol Pharmacol* **39**, 666–670.

Kinarsky L, Feng B, Skifter DA, Morley RM, Sherman S, Jane DE & Monaghan DT (2005). Identification of subunit- and antagonist-specific amino acid residues in the N-methyl-D-aspartate receptor glutamate-binding pocket. *J Pharmacol Exp Ther* **313**, 1066–1074.

Kleckner NW & Dingledine R (1988). Requirement for glycine in activation of NMDA-receptors expressed in *Xenopus* oocytes. *Science* **241**, 835–837.

Kristensen AS, Geballe MT, Snyder JP & Traynelis SF (2006). Glutamate receptors: variation in structure-function coupling. *Trends Pharmacol Sci* **27**, 65–69.

Kuryatov A, Laube B, Betz H & Kuhse J (1994). Mutational analysis of the glycine-binding site of the NMDA receptor: structural similarity with bacterial amino acid-binding proteins. *Neuron* **12**, 1291–1300.

Kutsuwada T, Kashiwabuchi N, Mori H, Sakimura K, Kushiya E, Araki K, Meguro H, Masaki H, Kumanishi T, Arakawa M *et al*. (1992). Molecular diversity of the NMDA receptor channel. *Nature* **358**, 36–41.

Laube B, Hirai H, Sturgess M, Betz H & Kuhse J (1997). Molecular deteminants of agonist discrimination by NMDA receptor subunits: analysis of the glutamate binding site on the NR2B subunit. *Neuron* **18**, 493–503.

Laurie DJ & Seeburg PH (1994). Regional and developmental heterogeneity in splicing of the rat brain NMDAR1 mRNA. *J Neurosci* **14**, 3180–3194.

Lee CJ, Mannaioni G, Yuan H, Woo DH, Gingrich MB & Traynelis SF (2007). Astrocytic control of synaptic NMDA receptors. *J Physiol* **581**, 1057–1081.

Lester RA, Tong G & Jahr CE (1993). Interactions between the glycine and glutamate binding sites of the NMDA receptor. *J Neurosci* **13**, 1088–1096.

Maier W, Schemm R, Grewer C & Laube B (2007). Disruption of inter-domain interactions in the glutamate binding pocket affects differentially agonist affinity and efficacy of N-methyl-D-aspartate receptor activation. *J Biol Chem* **282**, 1863–1872.

Mayer ML (2005). Crystal structures of the GluR5 and GluR6 ligand binding cores: molecular mechanisms underlying kainate receptor selectivity. *Neuron* **17**, 539–552.

Mayer ML (2006). Glutamate receptors at atomic resolution. *Nature* **440**, 456–462.

McNamara D, Smith EC, Calligaro DO, O'Malley PJ, McQuaid LA & Dingledine R (1990). 5,7-Dichlorokynurenic acid, a potent and selective competitive antagonist of the glycine site on NMDA receptors. *Neurosci Lett* **120**, 17–20.

Monyer H, Burnashev N, Laurie DJ, Sakmann B & Seeburg PH (1994). Developmental and regional expression in the rat brain and functional properties of four NMDA receptors. *Neuron* **12**, 529–540.

Monyer H, Sprengel R, Schoepfer R, Herb A, Higuchi M, Lomeli H, Burnashev N, Sakmann B & Seeburg PH (1992). Heteromeric NMDA receptors: Molecular and functional distinctions of subtypes. *Science* **256**, 1217–1221.

Nanao MH, Green T, Stern-Bach Y, Heinemann SF & Choe S (2005). Structure of the kainate receptor subunit GluR6 agonist-binding domain complexed with domoic acid. *Proc Natl Acad Sci U S A* **102**, 1708–1713.

Popescu G & Auerbach A (2003). Modal gating of NMDA receptors and the shape of their synaptic response. *Nat Neurosci* **6**, 476–483.

Priestley T & Kemp JA (1994). Kinetic study of the interactions between the glutamate and glycine recognition sites on the *N*-methyl-D-aspartic acid receptor complex. *Mol Pharmacol* **46**, 1191–1196.

Regalado MP, Villarroel A & Lerma J (2001). Intersubunit cooperativity in the NMDA receptor. *Neuron* **32**, 1085–1096.

Robert A, Armstrong N, Gouaux E & Howe JR (2005). AMPA receptor binding cleft mutations that alter affinity, efficacy, and recovery from desensitization. *J Neurosci* **25**, 3752–3762.

Schorge S, Elenes S & Colquhoun D (2005). Maximum likelihood fitting of single channel NMDA activity with a mechanism composed of independent dimers of subunits. *J Physiol* **569**, 395–418.

Supplisson S & Bergman C (1997). Control of NMDA receptor activation by a glycine transporter co-expressed in *Xenopus* oocytes. *J Neurosci* **17**, 4580–4590.

Thomson AM, Walker VE & Flynn DM (1989). Glycine enhances NMDA-receptor mediated synaptic potentials in neocortical slices. *Nature* **338**, 422–424.

Traynelis SF, Burgess MF, Zheng F, Lyuboslavsky P & Powers JL (1998). Control of voltage-independent zinc inhibition of NMDA receptors by the NR1 subunit. *J Neurosci* **18**, 6163–6175.

Traynelis SF, Hartley M & Heinemann SF (1995). Control of proton sensitivity of the NMDA receptor by RNA splicing and polyamines. *Science* **268**, 873–876.

Vicini S, Wang JF, Li JH, Zhu WJ, Wang YH, Luo JH, Wolfe BB & Grayson DR (1998). Functional and pharmacological differences between recombinant N-methyl-D-aspartate receptors. *J Neurophysiol* **79**, 555–566.

Vyklicky L Jr, Benveniste M & Mayer ML (1990). Modulation of N-methyl-D-aspartic acid receptor desensitization by glycine in mouse cultured hippocampal neurones. *J Physiol* **428**, 313–331.

Wafford KA, Kathoria M, Bain CJ, Marshall G, Le Bourdelles B, Kemp JA & Whiting PJ (1995). Identification of amino acids in the N-methyl-D-aspartate receptor NR1 subunit that contribute to the glycine binding site. *Mol Pharmacol* **47**, 374–380.

Weston MC, Gertler C, Mayer ML & Rosenmund C (2006). Interdomain interactions in AMPA and kainate receptors regulate affinity for glutamate. *J Neurosci* **26**, 7650–7658.

Williams K, Chao J, Kashiwagi K, Masuko T & Igarashi K (1996). Activation of N-methyl-D-aspartate receptors by glycine: Role of an aspartate residue in the M3–M4 loop of the NR1 subunit. *Mol Pharmacol* **50**, 701–708.

Wrighton DC, Baker EJ, Chen PE & Wyllie DJA (2008). Mg^{2+} and memantine block of rat recombinant NMDA receptors containing chimeric NR2A/2D subunits expressed in *Xenopus laevis* oocytes. *J Physiol* **586**, 211–225.

Wyllie DJA, Béhé P & Colquhoun D (1998). Single-channel activations and concentration jumps: comparison of recombinant NR1a/NR2A and NR1a/NR2D NMDA receptors. *J Physiol* **510**, 1–18.

Wyllie DJA, Béhé P, Nassar M, Schoepfer R & Colquhoun D (1996). Single-channel currents from recombinant NMDA NR1a/NR2D receptors expressed in *Xenopus* oocytes. *Proc Biol Sci* **263**, 1079–1086.

Wyllie DJA & Chen PE (2007). Taking the time to study competitive antagonism. *Br J Pharmacol* **150**, 541–551.

Wyllie DJA, Johnston AR, Lipscombe D & Chen PE (2006). Single-channel analysis of a point mutation of a conserved serine residue in the S2 ligand binding domain of the NR2A NMDA receptor. *J Physiol* **574**, 477–489.

Acknowledgements

Authors' present addresses

K. E. Erreger: Department of Molecular Physiology and Biophysics, Vanderbilt University, 465 21st Avenue, Nashville, TN 37232, USA.

M. R. Livesey: Neurosciences Institute, Division of Pathology and Neuroscience, Ninewells Hospital and Medical School, Dundee, DD1 9SY, UK.

C. J. Lee: Center for Neural Science, Division of Life Sciences, Korea Institute of Science and Technology, Seoul, Korea.

Supplemental material

Online supplemental material for this paper can be accessed at: http://jp.physoc.org/cgi/content/full/jphysiol.2007.143172/DC1 and
http://www.blackwell-synergy.com/doi/suppl/10.1113/jphysiol.2007.143172